

Higher order terms in the inflaton potential and the lower bound on the tensor to scalar ratio r

C. Destri*

*Dipartimento di Fisica G. Occhialini, Università Milano-Bicocca and INFN,
sezione di Milano-Bicocca, Piazza della Scienza 3, 20126 Milano, Italia.*

H. J. de Vega[†]

*LPTHE, Université Pierre et Marie Curie (Paris VI) et Denis Diderot (Paris VII),
Laboratoire Associé au CNRS UMR 7589, Tour 24, 5ème. étage,
Boite 126, 4, Place Jussieu, 75252 Paris, Cedex 05, France and
Observatoire de Paris, LERMA. Laboratoire Associé au CNRS UMR 8112,
61, Avenue de l'Observatoire, 75014 Paris, France.*

N. G. Sanchez[‡]

*Observatoire de Paris, LERMA. Laboratoire Associé au CNRS UMR 8112,
61, Avenue de l'Observatoire, 75014 Paris, France.*

(Dated: May 30, 2018)

The MCMC analysis of the CMB+LSS data in the context of the Ginsburg-Landau approach to inflation indicated that the fourth degree double-well inflaton potential in new inflation gives an excellent fit of the present CMB and LSS data. This provided a **lower bound** for the ratio r of the tensor to scalar fluctuations and as most probable value $r \simeq 0.05$, within reach of the forthcoming CMB observations. In this paper we systematically analyze the effects of arbitrarily **higher order** terms in the inflaton potential on the CMB observables: spectral index n_s and ratio r . Furthermore, we compute in close form the inflaton potential dynamically generated when the inflaton field is a fermion condensate in the inflationary universe. This inflaton potential turns out to belong to the Ginsburg-Landau class too. The theoretical values in the (n_s, r) plane for all double well inflaton potentials in the Ginsburg-Landau approach (including the potential generated by fermions) fall inside a **universal** banana-shaped region \mathcal{B} . The upper border of the banana-shaped region \mathcal{B} is given by the fourth order double-well potential and provides an upper bound for the ratio r . The lower border of \mathcal{B} is defined by the quadratic plus an infinite barrier inflaton potential and provides a **lower bound** for the ratio r . For example, the current best value of the spectral index $n_s = 0.964$, implies r is in the interval: $0.021 < r < 0.053$. Interestingly enough, this range is within reach of forthcoming CMB observations.

Contents

I. Introduction	2
II. Physical parametrization for inflaton potentials	4
A. The fourth degree double-well inflaton potential	7
B. The sixth-order double-well inflaton potential	8
III. Higher-order even polynomial double-well inflaton potentials	10
IV. The quadratic plus the $2n$ th order double-well inflaton potential	12
A. The $n \rightarrow \infty$ limit at fixed u .	14
B. The double limit $n \rightarrow \infty$ and $u \rightarrow 1$.	15
V. The quadratic plus the exponential potential.	16
A. The limit $b \rightarrow \infty$ at fixed u .	17
B. The double limit $b \rightarrow \infty$ and $u \rightarrow 1$.	18
VI. Dynamically generated inflaton potential from a fermion condensate in the inflationary stage.	19

*Electronic address: Claudio.Destri@mib.infn.it

[†]Electronic address: devega@lpthe.jussieu.fr

[‡]Electronic address: Norma.Sanchez@obspm.fr

I. INTRODUCTION

The current WMAP data are validating the single field slow-roll scenario [1]. Single field slow-roll models provide an appealing, simple and fairly generic description of inflation [2, 3]. This inflationary scenario can be implemented using a scalar field, the *inflaton* with a Lagrangian density

$$\mathcal{L} = a^3(t) \left[\frac{\dot{\varphi}^2}{2} - \frac{(\nabla\varphi)^2}{2a^2(t)} - V(\varphi) \right], \quad (1.1)$$

where $V(\varphi)$ is the inflaton potential. Since the universe expands exponentially fast during inflation, gradient terms are exponentially suppressed and can be neglected. At the same time, the exponential stretching of spatial lengths classicalize the physics and permits a classical treatment. One can therefore consider an homogeneous and classical inflaton field $\varphi(t)$ which obeys the evolution equation

$$\ddot{\varphi} + 3H(t)\dot{\varphi} + V'(\varphi) = 0, \quad (1.2)$$

in the isotropic and homogeneous Friedmann-Robertson-Walker (FRW) metric

$$ds^2 = dt^2 - a^2(t) d\vec{x}^2, \quad (1.3)$$

which is sourced by the inflaton. Here $H(t) \equiv \dot{a}(t)/a(t)$ stands for the Hubble parameter. The energy density and the pressure for a spatially homogeneous inflaton are given by

$$\rho = \frac{\dot{\varphi}^2}{2} + V(\varphi), \quad p = \frac{\dot{\varphi}^2}{2} - V(\varphi). \quad (1.4)$$

The scale factor $a(t)$ obeys the Friedmann equation,

$$H^2(t) = \frac{1}{3M_{Pl}^2} \left[\frac{1}{2} \dot{\varphi}^2 + V(\varphi) \right]. \quad (1.5)$$

In order to have a finite number of inflation e-folds, the inflaton potential $V(\varphi)$ must vanish at its absolute minimum

$$V'(\varphi_{min}) = V(\varphi_{min}) = 0. \quad (1.6)$$

These two conditions guarantee that inflation is not eternal. Since the inflaton field is space-independent inflation is followed by a matter dominated era (see for example ref. [7]).

Inflation as known today should be considered as an **effective theory**, that is, it is not a fundamental theory but a theory of a condensate (the inflaton field) which follows from a more fundamental one. In order to describe the cosmological evolution it is enough to consider the effective dynamics of such condensates. The inflaton field ϕ may **not** correspond to any real particle (even unstable) but is just an **effective** description while the microscopic description should come from a Grand Unification theory (GUT) model.

At present, there is no derivation of the inflaton model from a microscopic GUT theory. However, the relation between the effective field theory of inflation and the microscopic fundamental theory is akin to the relation between the effective Ginsburg-Landau theory of superconductivity [4] and the microscopic BCS theory, or like the relation of the $O(4)$ sigma model, an effective low energy theory of pions, photons and nucleons (as skyrmions), with the corresponding microscopic theory: quantum chromodynamics (QCD).

In the absence of a microscopic theory of inflation, we find that the Ginsburg-Landau approach is a powerful effective theory description. Such effective approach has been fully successful in several branches of physics when the microscopic theory is not available or when it is very complicated to solve in the regime considered. This is the case in statistical physics, particle physics and condensed matter physics. Such GL effective theory approach permits to analyse the physics in a quantitative way without committing to a specific model [4].

The Ginsburg-Landau framework is not just a class of physically well motivated inflaton potentials, among them the double and single well potentials. The Ginsburg-Landau approach provides the effective theory for inflation, with powerful gain in the physical insight and analysis of the data. As explained in this paper and shown in the refs. [6]-[7], the analysis of the present set of CMB+LSS data with the effective theory of inflation, favor the double well potential. Of course, just analyzing the present data without this powerful physical theory insight, does not allow to

discriminate between classes of models, and so, very superficially and incompletely, it would seem that almost all the potentials are still at the same footing, waiting for the new data to discriminate them.

In the Ginsburg-Landau spirit the potential is a polynomial in the field starting by a constant term [4]. Linear terms can always be eliminated by a constant shift of the inflaton field. The quadratic term can have a positive or a negative sign associated to unbroken symmetry (chaotic inflation) or to broken symmetry (new inflation), respectively.

As shown in refs. [6, 7] a negative quadratic term and a negligible cubic term in new inflation provides a very good fit to the CMB+LSS data, (the inflaton starts at or very close to the false vacuum $\varphi = 0$). The analysis in refs.[6, 7] showed that chaotic inflation is clearly disfavoured compared with new inflation. Namely, inflaton potentials with $V''(0) < 0$ are favoured with the inflaton starting to evolve at $\varphi = 0$.

We can therefore ignore the linear and cubic terms in $V(\varphi)$. If we restrict ourselves for the moment to fourth order polynomial potentials, eq.(1.6) and $V''(0) < 0$ imply that the inflaton potential is a double well (broken symmetric) with the following form:

$$V(\varphi) = -\frac{1}{2} m^2 \varphi^2 + \frac{1}{4} \lambda \varphi^4 + \frac{m^4}{4\lambda} = \frac{1}{4} \lambda \left(\varphi^2 - \frac{m^2}{\lambda} \right)^2. \quad (1.7)$$

The mass term m^2 and the coupling λ are naturally expressed in terms of the **two** energy scales which are relevant in this context: the energy scale of inflation M and the Planck mass $M_{Pl} = 2.43534 \cdot 10^{18}$ GeV,

$$m = \frac{M^2}{M_{Pl}}, \quad \lambda = \frac{y}{8N} \left(\frac{M}{M_{Pl}} \right)^4. \quad (1.8)$$

Here $y = \mathcal{O}(1)$ is the quartic coupling.

The MCMC analysis of the CMB+LSS data combined with the theoretical input above yields the value $y \simeq 1.26$ for the coupling [6, 7]. y turns out to be **order one** consistent with the Ginsburg-Landau formulation of the theory of inflation [7].

According to the current CMB+LSS data, this fourth order double-well potential of new inflation yields as most probable values: $n_s \simeq 0.964$, $r \simeq 0.051$ [6, 7]. This value for r is within reach of forthcoming CMB observations [21]. For the best fit value $y \simeq 1.26$, the inflaton field exits the horizon in the negative concavity region $V''(\varphi) < 0$ intrinsic to new inflation. We find for the best fit [6, 7],

$$M = 0.543 \times 10^{16} \text{ GeV for the scale of inflation and } m = 1.21 \times 10^{13} \text{ GeV for the inflaton mass.} \quad (1.9)$$

It must be stressed that in our approach the amplitude of scalar fluctuations $|\Delta_{k ad}^{\mathcal{R}}| = (4.94 \pm 0.1) \times 10^{-5}$ allows us to completely determine the energy scale of inflation which turns out to coincide with the Grand Unification energy scale (well below the Planck energy scale). Namely, we succeed to derive the energy scale of inflation without the knowledge of the value of r from observations. $M \ll M_{Pl}$ guarantees the validity of the effective theory approach to inflation. The fact that the inflaton mass is $m \ll M$ implies the appearance of infrared phenomenon as the quasi-scale invariance of the primordial power.

Since the inflaton potential must be bounded from below $V(\varphi) \geq 0$, the highest degree term must be even and with a positive coefficient. Hence, we consider polynomial potentials of degree $2n$ where $1 < n \leq \infty$.

The request of renormalizability restricts the degree of the inflaton potential to four. However, since the theory of inflation is an effective theory, potentials of degrees higher than four are in principle acceptable.

A given Ginsburg-Landau potential will be **reliable** provided it is **stable** under the addition to the potential of terms of higher order. Namely, adding to the $2n$ th order potential further terms of order $2n+1$ and $2n+2$ should only produce **small** changes in the observables. Otherwise, the description obtained could not be trusted. Since, the highest degree term must be even and positive, this implies that all even terms of order higher or equal than four should be positive.

Moreover, when expressed in terms of the appropriate dimensionless variables, a relevant dimensionless coupling constant g can be defined by rescaling the inflaton field. This coupling g turns out to be of order $1/N$ where $N \sim 60$ is the number of e-folds since the cosmologically relevant modes exit the horizon till the end of inflation showing that the slow-roll approximation is in fact an expansion in $1/N$ [5]. It is then natural to introduce as coupling constant $y \equiv 8N g = \mathcal{O}(N^0)$. This is consistent with the stability of the results in the above sense. Generally speaking, the Ginsburg-Landau approach makes sense for small or moderate coupling.

Odd terms in the inflaton field φ are allowed in $V(\varphi)$ in the effective theory of inflation. Choosing $V(\varphi)$ an even function of φ implies that $\varphi \rightarrow -\varphi$ is a symmetry of the inflaton potential. At the moment, as stated in [7, 12], we do not see reasons based on fundamental physics to choose a zero or a nonzero cubic term, which is the first non-trivial odd term. Only the phenomenology, that is the fit to the CMB+LSS data, decides on the value of the cubic and the higher order odd terms. The MCMC analysis of the WMAP plus LSS data shows that the cubic term is negligible and therefore can be ignored for new inflation [6, 7]. CMB data have also been analyzed at the light of slow-roll inflation in refs. [8].

In the present paper we systematically study the effects produced by higher order terms ($n > 4$) in the inflationary potential on the observables n_s and r .

We show in this paper that all $r = r(n_s)$ curves for a large class of double-well potentials of arbitrary high order in new inflation fall **inside** the **universal** banana region \mathcal{B} depicted in fig. 10. Moreover, we find that the $r = r(n_s)$ curves for even double-well potentials with arbitrarily positive higher order terms lie **inside** the universal banana region \mathcal{B} [fig. 10]. This is true for arbitrarily large values of the coefficients in the potential.

Furthermore, the inflaton field may be a condensate of fermion-antifermion pairs in a grand unified theory (GUT) in the inflationary background. In this paper we explicitly write down in closed form the inflaton potential dynamically generated as the effective potential of fermions in the inflationary universe. This inflaton potential turns out to belong to the Ginsburg-Landau class of potentials considered in this paper. We find that the corresponding $r = r(n_s)$ curves lie inside the **universal** banana region \mathcal{B} provided the one-loop part of the inflaton potential is at most of the same order as the tree level piece. Therefore, a **lower bound** for the ratio tensor/scalar fluctuations r is present for **all** potentials above mentioned. For the current best value of the spectral index $n_s = 0.964$ [1, 7] the lower bound turns out to be $r > 0.021$.

Namely, the shape of the banana region fig. 10 **combined** with the value $n_s = 0.964$ for the spectral index yields the lower bound $r > 0.021$. If one consider low enough values for n_s (in disagreement with observations) r can be arbitrarily small within the GL class of inflaton potentials.

The upper border of the universal region \mathcal{B} tells us that $r < 0.053$ for $n_s = 0.964$. Therefore, we have inside the region \mathcal{B} within the large class of potentials considered here

$$0.021 < r < 0.053 \quad \text{for} \quad n_s = 0.964 .$$

Interestingly enough $r \simeq 0.04$ is within reach, although borderline for the Planck satellite [21].

Among the simplest potentials in the Ginsburg-Landau class, the one that best reproduces the present CMB+LSS data, is the fourth order double-well potential eq.(1.7), yielding as most probable values: $n_s \simeq 0.964$, $r \simeq 0.051$. Our work here shows that adding higher order terms to the inflaton potential does not really improve the data description in spite of the addition of new free parameters. Therefore, the fourth order double-well potential gives a robust and stable description of the present CMB/LSS data and provides clear predictions to be contrasted with the forthcoming CMB observations [21].

There is an abundant literature on slow-roll inflationary potentials and the cosmological parameters n_s and r including new inflation and in particular hilltop inflation [13–16].

The question on whether a lower bound for r is found or not depends on whether the Ginsburg-Landau (G-L) effective field approach to inflation is used or not. Namely, within the G-L approach, the new inflation double well potential determines a banana shaped relationship $r = r(n_s)$ which for the observed n_s value determines a lower bound on r . The analysis of the CMB+LSS data within the G-L approach which we performed in refs. [6, 7] shows that new inflation is preferred by the data with respect to chaotic inflation for fourth degree potentials, and that the lower bound on r is then present. Without using the powerful physical G-L framework such discrimination between the two classes of inflation models is not possible and the lower bound for r does not emerge. Other references in the field (i. e. [13, 19, 20]) do not work within the Ginsburg-Landau framework, do not find lower bounds for r and cannot exclude arbitrarily small values for r , much smaller than our lower bound $r \simeq 0.021$.

This paper is organized as follows: in section II we present in general inflaton potentials of arbitrary high degree, specializing then to fourth and sixth-order polynomial potentials and displaying their corresponding $r = r(n_s)$ curves. Sec. III contains the $2n$ th order double-well polynomial inflaton potentials with arbitrary random coefficients and their $r = r(n_s)$ curves. Sec. IV presents the $n \rightarrow \infty$ limits of these polynomial potentials and we present in sec. V the exponential potential and its infinite coupling limit. In sec. V we compute the inflaton potential from dynamically generated fermion condensates in a de Sitter space-time displaying their $r = r(n_s)$ curves. Finally, we present and discuss the universal banana region in sec. VII together with our conclusions.

II. PHYSICAL PARAMETRIZATION FOR INFLATON POTENTIALS

We start by writing the inflaton potential in dimensionless variables as [12]

$$V(\varphi) = M^4 v \left(\frac{\varphi}{M_{Pl}} \right) , \quad (2.1)$$

where M is the energy scale of inflation and $v(\phi)$ is a dimensionless function of the dimensionless field argument $\phi = \varphi/M_{Pl}$. Without loss of generality we can set $v'(0) = 0$. Moreover, provided $V''(0) \neq 0$ we can choose without loss of generality $|v''(0)| = 1/2$.

In the slow-roll regime, higher time derivatives in the equations of motion can be neglected with the final well known result for the number of efolts

$$N = - \int_{\phi_{exit}}^{\phi_{end}} d\phi \frac{v(\phi)}{v'(\phi)}, \quad (2.2)$$

where ϕ_{exit} is the inflaton field at horizon exit. To leading order in $1/N$ we can take ϕ_{end} to be the value ϕ_{min} at which $v(\phi)$ attains its absolute minimum $v(\phi_{min})$, which must be zero since inflation must stop after a finite number of efolts [7].

Then, in chaotic inflation we have $\phi_{min} = 0$, with $v'(\phi) > 0$ for $\phi > 0$, while in new inflation we have $\phi_{min} > 0$ with $v'(\phi) < 0$ for $0 < \phi < \phi_{min}$. We consider potentials $v(\phi)$ that can be expanded in Taylor series around $\phi = \phi_{min}$, with a non-vanishing quadratic (mass) term.

It is convenient to rescale the inflaton field in order to conveniently parametrize the higher order potential. We define a coupling parameter $g > 0$ by rescaling the inflaton and its potential keeping invariant the quadratic term, that is

$$v(\phi) = \frac{1}{g} v_1(\phi \sqrt{g}) \quad (2.3)$$

For a potential $v_1(u)$ expanded in power series around $u = 0$ we write:

$$v_1(u) = c_0 \mp \frac{1}{2} u^2 + \sum_{k \geq 3} \frac{c_k}{k} u^k \quad (2.4)$$

Then, replacing

$$u = \phi \sqrt{g}, \quad (2.5)$$

we find

$$v(\phi) = \frac{c_0}{g} \mp \frac{1}{2} \phi^2 + \sum_{k \geq 3} \frac{g^{k/2-1}}{k} c_k \phi^k. \quad (2.6)$$

The positive sign in the quadratic term corresponds to chaotic inflation (in which case $c_0 = 0$), while the negative sign corresponds to new inflation (in which case c_0 is chosen such that $v_1(u)$ vanishes at its absolute minimum).

Clearly g plus the set of coefficients c_k provide an overcomplete parametrization of the inflaton potential which we will now reduce. In the case of chaotic inflation a convenient choice is $c_4 = 1$, so that

$$v(\phi) = \frac{1}{2} \phi^2 + \sqrt{g} \frac{c_3}{3} \phi^3 + \frac{g}{4} \phi^4 + \sum_{k \geq 5} \frac{g^{k/2-1}}{k} c_k \phi^k \quad [\text{chaotic inflation}] \quad (2.7)$$

which represents a generic higher order perturbation of the trinomial chaotic inflation studied in refs. [6].

In the case of new inflation, where $\phi_{min} > 0$, it is more convenient to set without loss of generality that $u_{min} = 1$, $\phi_{min} = 1/\sqrt{g}$. In order to have appropriate inflation, $u_{min} = 1$ must be the absolute minimum of $v_1(u)$ and the closest one to the origin on the positive semi-axis. That is,

$$v'_1(1) = -1 + \sum_{k \geq 3} c_k = 0 \quad (2.8)$$

and then $v_1(1) = 0$ fixes from eq.(2.3) the constant term c_0 in the potential

$$c_0 = \frac{1}{2} - \sum_{k \geq 3} \frac{c_k}{k} \quad (2.9)$$

We thus get for the inflaton potential

$$v_1(u) = \frac{1}{2}(1 - u^2) + \sum_{k \geq 3} \frac{c_k}{k} (u^k - 1) \quad [\text{new inflation}], \quad (2.10)$$

corresponding to

$$v(\phi) = \frac{1}{2} \left(\frac{1}{g} - \phi^2 \right) + \sum_{k \geq 3} \frac{c_k}{k} \left(g^{k/2-1} \phi^k - \frac{1}{g} \right) \quad [\text{new inflation}] \quad (2.11)$$

For the coupling g and the field ϕ using eq.(2.5),

$$g = \frac{1}{\phi_{min}^2} = \frac{M_{Pl}^2}{\varphi_{min}^2} \quad , \quad u = \frac{\phi}{\phi_{min}} = \frac{\varphi}{\varphi_{min}} \quad . \quad (2.12)$$

From eq.(2.2) it now follows that the parameter g can be expressed as the integral

$$y(u) = 8 \int_{u_{min}}^u dx \frac{v_1(x)}{v_1'(x)} \quad , \quad u \equiv \sqrt{g} \phi_{exit} \quad , \quad (2.13)$$

where,

$$g = \frac{y(u)}{8N} \quad , \quad (2.14)$$

with $u_{min} = 0$ for chaotic inflation and $u_{min} = 1$ for new inflation. Eq.(2.13) can be regarded as a parametrization of g and $y(u)$ in terms of the rescaled exit field u . Clearly, *as a function of u* , g is uniformly of order $1/N$. g is numerically of order $1/N$ as long as $y(u)$ is of order one. As we shall see, typically both u at horizon exit and $y(u)$ are of order one. We have $0 < u < 1$ for new inflation and $0 < u < +\infty$ for chaotic inflation.

In what follows we therefore use $y(u)$ instead of g as a **coupling constant** and make contact with eq.(2.1) by setting

$$\varphi = M_{Pl} \sqrt{\frac{8N}{y}} u \quad , \quad V(\varphi) = \frac{8N M^4}{y} v_1 \left(\sqrt{\frac{y}{8N}} \frac{\varphi}{M_{Pl}} \right) \quad . \quad (2.15)$$

We can easily read from this equation the order of magnitude of φ and $V(\varphi)$ since $N \sim 60$, M is given by eq.(1.9) and u and y are of order one. Hence, $\varphi \sim M_{Pl}$ and $V(\varphi) \sim N M^4$.

As we will see below, the coupling y (or g) is the most relevant coupling since it is related to the inflaton rescaling: the tensor-scalar ratio r and the spectral index n_s vary in a more relevant manner with y than with the rest of the parameters c_k , $k \geq 3$ in the potential eq.(2.6).

By construction the function $y(u)$ has the following properties

- $y(u) > 0$;
- $y'(u) > 0$ for $u > 0$ in chaotic inflation;
- $y'(u) < 0$ for $0 < u < u_{min} = 1$ in new inflation;
- $y(u) = 2(u - u_{min})^2 + \mathcal{O}(u - u_{min})^3 \rightarrow 0$ as $u \rightarrow u_{min}$;
- $y(u) \rightarrow \infty$ as $u \rightarrow \infty$ in chaotic inflation;
- $y(u) \simeq -8 v_1(0) \log u \rightarrow +\infty$ as $u \rightarrow 0^+$ in new inflation.

In terms of this parametrization and to leading order in $1/N$, the tensor to scalar ratio r and the spectral index n_s read:

$$r = \frac{y(u)}{N} \left[\frac{v_1'(u)}{v_1(u)} \right]^2 \quad , \quad n_s - 1 = -\frac{3}{8} r + \frac{y(u)}{4N} \frac{v_1''(u)}{v_1(u)} \quad (2.16)$$

Notice that both $n_s - 1$ and r are of order $1/N$ for generic inflation potentials in this Ginsburg-Landau framework as we see from eq.(2.16). Moreover, the running of the scalar spectral index from eq.(2.15) and its slow-roll expression turn out to be of order $1/N^2 \sim 1/3600 \sim 3 \times 10^{-4} \ll 1$

$$\frac{dn_s}{d \ln k} = -\frac{y^2(u)}{32 N^2} \left\{ \frac{v_1'(u) v_1'''(u)}{v_1^2(u)} + 3 \frac{[v_1'(u)]^4}{v_1^4(u)} - 4 \frac{[v_1'(u)]^2 v_1''(u)}{v_1^3(u)} \right\} \quad .$$

and therefore can be neglected [7]. Such small estimate for $dn_s/d \log k$ is in agreement with the present data [1] and makes the running unobservable for a foreseeable future.

Since $y = y(u)$ can be inverted for any $0 < u < u_{min}$, these two relations can also be regarded as parametrizations $r = r(y)$ and $n_s = n_s(y)$ in terms of the coupling constant y .

We are interested in the region of the (n_s, r) plane obtained from eq.(2.16) by varying y (or u) and the other parameters in the inflaton potential. We call \mathcal{B} this region.

From now on, we will restrict to new inflation.

For a generic $v_1(u)$ [with the required global properties described above] we can determine the asymptotic of \mathcal{B} , since they follow from the weak coupling limit $y \rightarrow 0$ and from the strong coupling limit $y \rightarrow \infty$. When $y \rightarrow 0$, then $u \rightarrow u_{min} = 1$ and from the property above,

$$r = \frac{8}{N} + \mathcal{O}(u - 1) = 0.13333 \dots + \mathcal{O}(u - 1) \quad (2.17)$$

and

$$n_s = 1 - \frac{2}{N} + \mathcal{O}(u - 1) = 0.9666 \dots + \mathcal{O}(u - 1) . \quad (2.18)$$

When $y \rightarrow \infty$ we have in new inflation $u \rightarrow 0$ and then,

$$n_s \simeq 1 + \frac{2}{N} \log u \longrightarrow -\infty \quad , \quad r \simeq -\frac{8}{N} \frac{u^2 \log u}{v_1(0)} \longrightarrow 0^+ . \quad (2.19)$$

We see that in the strong coupling regime r becomes very small and n_s becomes well below unity. However, the slow-roll approximation is valid for $|n_s - 1| < 1$ and in any case, the WMAP+LSS results exclude $n_s < 0.9$ [1]. Therefore, the strong coupling limit is ruled out.

Eq.(2.16) for r can be rewritten using eq.(2.13) in the suggestive form,

$$r = \frac{64}{N y(u)} \left[\frac{d \ln y(u)}{du} \right]^{-2} \quad (2.20)$$

Since $64/N \sim 1$, r may be **small** only in case $y(u)$ is **large** (the logarithmic derivative of $y(u)$ has a milder effect for large $y(u)$.) Therefore, we only find $r \ll 1$ in a **strong** coupling regime. Notice that φ is much smaller than M_{Pl} in the strong coupling regime [eq.(2.12)].

Let us now study large classes of physically meaningful inflaton potentials in order to provide generic bounds on the region \mathcal{B} of the (n_s, r) plane within an interval of n_s surely compatible with the WMAP+LSS data for n_s , namely $0.93 < n_s < 0.99$. To gain insight into the problem, we consider first the cases amenable to an analytic treatment, leaving the generic cases to a numerical investigation. As we will see below, the boundaries of the region \mathcal{B} turn out to be described parametrically by the analytic formulas (2.23) and (4.6).

A. The fourth degree double-well inflaton potential

The case when the $V(\varphi)$ is the standard double-well quartic polynomial

$$V(\varphi) = \frac{1}{4} \lambda \left(\varphi^2 - \frac{m^2}{\lambda} \right)^2$$

has been studied in refs. [6, 7]. In the general framework outlined above we have for this case,

$$v_1(u) = \frac{1}{4} (u^2 - 1)^2 = \frac{1}{4} - \frac{1}{2} u^2 + \frac{1}{4} u^4, \quad \lambda = \frac{y}{8N} \left(\frac{M}{M_{Pl}} \right)^4, \quad m = \frac{M^2}{M_{Pl}} . \quad (2.21)$$

By explicitly evaluating the integral in eq. (2.13) one obtains

$$y(u) = u^2 - 1 - \log u^2, \quad (2.22)$$

and then, from eq. (2.16)

$$n_s = 1 - \frac{1}{N} \frac{3u^2 + 1}{(1 - u^2)^2} (u^2 - 1 - \log u^2), \quad r = \frac{1}{N} \frac{16u^2}{(1 - u^2)^2} (u^2 - 1 - \log u^2) \quad (2.23)$$

where $0 \leq u \leq u_{min} = 1$. As required by the general arguments above, u is a monotonically decreasing function of y , ranging from $u = 1$ till $u = 0$ when y increases from $y = 0$ till $y = +\infty$. In particular, when $u \rightarrow 1^-$, y vanishes quadratically as,

$$y(u) \stackrel{u \rightarrow 1^-}{\simeq} \frac{1}{2} (1 - u^2)^2 .$$

The concavity of the potential eq.(2.21) for the inflaton field at horizon crossing takes the value

$$v_1''(u) = 3 u^2 - 1 .$$

We see that $v_1''(u)$ vanishes at $u = 1/\sqrt{3}$, that is at $y = \ln 3 - 2/3 = 0.431946\dots$ (This is usually called the spinodal point [17]). Therefore,

$$v_1''(u) > 0 \quad \text{for } y < 0.431946\dots \quad \text{and} \quad v_1''(u) < 0 \quad \text{for } y > 0.431946\dots . \quad (2.24)$$

Our MCMC analysis of the CMB+LSS data combined with the theoretical model eq.(2.21) yields $y \simeq 1.26$ [6, 7] deep in the **negative** concavity region $v_1''(u) < 0$.

The negative concavity case $v_1''(u) < 0$ for $y > 0.431946\dots$ is **specific** to new inflation eq.(2.21). $v_1''(u)$ can be expressed as a linear combination of the observables n_s and r as

$$n_s - 1 + \frac{3}{8} r = \frac{y(u)}{4N} \frac{v_1''(u)}{v_1(u)}$$

As expected in the general framework presented above, the limit $u \rightarrow 1^-$ implies weak coupling $y \rightarrow 0^+$, that is, the potential is quadratic around the absolute minimum $u_{min} = 1$ and we find,

$$n_s \stackrel{y \rightarrow 0}{=} 1 - \frac{2}{N} \quad , \quad r \stackrel{y \rightarrow 0}{=} \frac{8}{N} \quad , \quad u \stackrel{y \rightarrow 0}{=} 1 \quad , \quad (2.25)$$

which coincide with n_s and r for the monomial quadratic potential in chaotic inflation.

In the limit $u \rightarrow 0^+$ which implies $y \rightarrow +\infty$ (strong coupling), we have

$$u \stackrel{y \rightarrow +\infty}{=} e^{-(y+1)/2} \rightarrow 0^+$$

and

$$n_s \stackrel{y \gg 1}{=} 1 - \frac{y}{N} \quad , \quad r \stackrel{y \gg 1}{=} \frac{16 y}{N} e^{-y-1} . \quad (2.26)$$

Notice that the slow-roll approximation is no longer valid when the coefficient of $1/N$ becomes much larger than unity. Hence, the results in eq.(2.26) are valid for $y \lesssim N$. We see that in this strong coupling regime (see fig. 1), r becomes very small and n_s becomes well below unity. However, the WMAP+LSS results exclude $n_s \lesssim 0.9$ [1]. Therefore, this strong coupling limit $y \gg 1$ is ruled out.

For the fourth order double-well inflaton potential, the relation $r = r(n_s)$ defined by eq.(2.23) is a single curve depicted with dotted lines in fig. 1. It represents the upper border of the banana shaped region \mathcal{B} in fig. 1.

Notice that there is here a maximum value for n_s , namely $n_s^{max} = 0.96782\dots$ with $r(n_s^{max}) = 0.1192\dots$ [7]. The curve $r = r(n_s)$ has here **two branches**: the lower branch $r < r(n_s^{max})$ in which r **increases** with increasing n_s and the upper branch $r > r(n_s^{max})$ in which r **decreases** with increasing n_s .

B. The sixth-order double-well inflaton potential

We consider here new inflation described by a six degree even polynomial potential with broken symmetry. According to eq. (2.1) and eq. (2.3) we then have

$$V(\varphi) = \frac{M^4}{g} v_1 \left(\frac{\sqrt{g} \varphi}{M_{Pl}} \right) , \quad v_1(u) = c_0 - \frac{1}{2} u^2 + \frac{c_4}{4} u^4 + \frac{c_6}{6} u^6 . \quad (2.27)$$

where for stability we assume $c_6 \geq 0$. Moreover, if we regard this case as a higher order correction to the quartic double-well potential, then c_4 is positive.

The inflaton potential eq.(2.27) is a particular case of eq.(2.4). The conditions eqs. (2.8) and (2.9) that the absolute minimum of $v_1(u)$ be at $u_{min} = 1$ yields

$$c_4 + c_6 = 1 \quad , \quad c_0 = \frac{1}{2} - \frac{1}{4} c_4 - \frac{1}{6} c_6 \quad (2.28)$$

It is convenient to use $b \equiv c_6$ as free parameter so that $b \geq 0$ and $c_4 = 1 - b$. Thus,

$$v_1(u) = \frac{1}{2} (1 - u^2) - \frac{1-b}{4} (1 - u^4) - \frac{b}{6} (1 - u^6) = \frac{1}{12} (1 - u^2)^2 (3 + b + 2 b u^2) \quad (2.29)$$

where $b \leq 1$ in order to ensure that $c_4 \geq 0$.

The integral in eq. (2.13) can be explicitly evaluated with the result

$$y(u) = 8 \int_1^u dx \frac{v_1(x)}{v_1'(x)} = \frac{2}{3} (u^2 - 1) - \frac{1}{3} (3 + b) \log u^2 + \frac{(1 + b)^2}{3b} \log \frac{1 + b u^2}{1 + b} \quad (2.30)$$

According to the general arguments presented above [see the lines below eq. (2.13)] one can verify that $y(u)$ is a monotonically decreasing function of u for $0 < u < 1$, where $+\infty > y > 0$.

The scalar index n_s and the tensor–scalar ratio r are evaluated from eq. (2.16) as

$$r = \frac{y}{N} \left[\frac{12 u (1 + b u^2)}{(1 - u^2)(3 + b + 2 b u^2)} \right]^2, \quad n_s = 1 - \frac{3}{8} r + \frac{3 y(u)}{N} \frac{5 b u^4 + 3(1 - b) u^2 - 1}{(1 - u^2)^2 (3 + b + 2 b u^2)} \quad (2.31)$$

Various curves $r = r(n_s)$ are plotted in fig. 1 for several values of b in the interval $[0, 1]$ sweeping the region \mathcal{B} . We see that for increasing b [namely, for increasing sextic coupling and decreasing quartic coupling, see eq.(2.29)] the curves move down and right, sweeping the banana-shape region \mathcal{B} depicted on fig. 1.

Clearly, y is a variable more **relevant** than b . Changing y moves n_s and r in the whole available range of values, while changing b only amounts to displacements **transverse** to the banana region \mathcal{B} in the n_s, r plane. In particular, for a given n_s , r becomes smaller for increasing b .

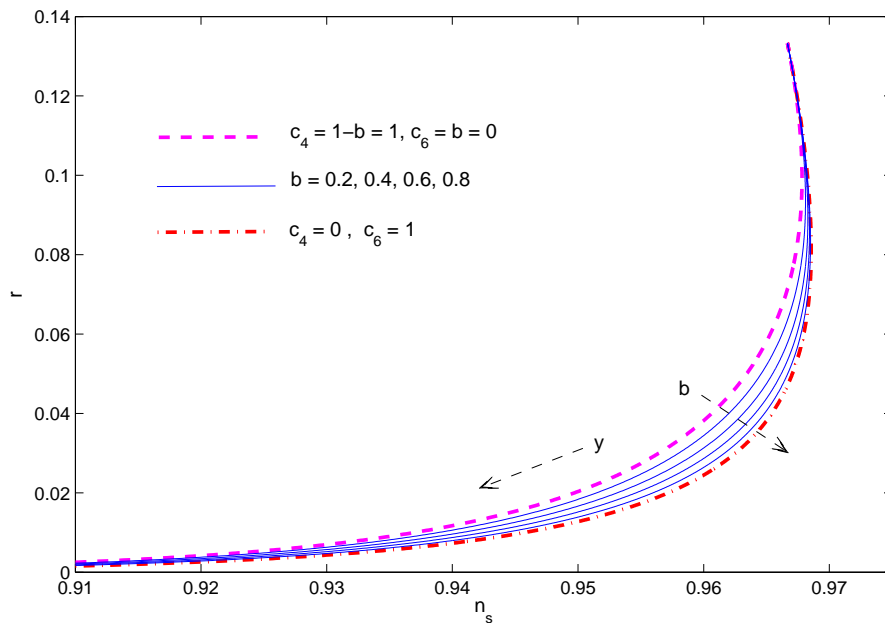


FIG. 1: We plot here r vs. n_s for the broken–symmetry sixth–order inflaton potential eq.(2.29) setting $N = 60$. The curves are obtained from eq. (2.31) with the sextic coefficient $b \equiv c_6$ fixed to the values indicated in the figure. We see that y is the relevant coupling while b only varies r and n_s transversely to the narrow banana-shape region. The two important limiting curves are shown: $b = 0$ corresponding to the fourth degree potential eq.(2.21) and $b = 1$ corresponding to the sixth degree potential eq.(2.32). The uppermost point where all curves coalesce corresponds to the monomial quadratic potential $n_s = 0.9666\dots$, $r = 0.13333\dots$ for $N = 60$ [see eqs.(2.17)-(2.18)].

We see in fig. 1 two important **limiting** curves: the $b \rightarrow 0$ and the $b \rightarrow 1$ curves. When $b = 0$ the function $v_1(u)$ reduces to the fourth order double-well potential eq.(2.21) and we recover its characteristic curve $r = r(n_s)$. When $b = 1$ the potential has no quartic term and reduces to the quadratic plus sixth order potential:

$$v_1(u) \stackrel{b \rightarrow 1}{\equiv} \frac{1}{6} (1 - u^2)^2 (2 + u^2) = \frac{1}{3} - \frac{1}{2} u^2 + \frac{1}{6} u^6. \quad (2.32)$$

In summary, the quadratic plus quartic broken–symmetry potential describes the upper/left border of the banana-shaped region \mathcal{B} of fig. 1, while the quadratic plus sextic broken–symmetry potential describes its lower/right border.

III. HIGHER-ORDER EVEN POLYNOMIAL DOUBLE-WELL INFLATON POTENTIALS

The generalization of the sixth order inflaton potential with broken symmetry to arbitrarily higher orders is now straightforward:

$$V(\varphi) = \frac{M^4}{g} v_1 \left(\frac{\sqrt{g} \varphi}{M_{Pl}} \right), \quad v_1(u) = \frac{1}{2} (1 - u^2) + \sum_{k=2}^n \frac{c_{2k}}{2k} (u^{2k} - 1), \quad (3.1)$$

with the constraint eq.(2.8)

$$\sum_{k=2}^n c_{2k} = 1 \quad (3.2)$$

which guarantees that $u = 1$ is an extreme of $v_1(u)$.

We consider here the case when all higher coefficients c_{2k} are positive or zero :

$$c_{2k} \geq 0, \quad k = 2, \dots, n$$

such that $u_{min} = 1$ is the unique positive minimum.

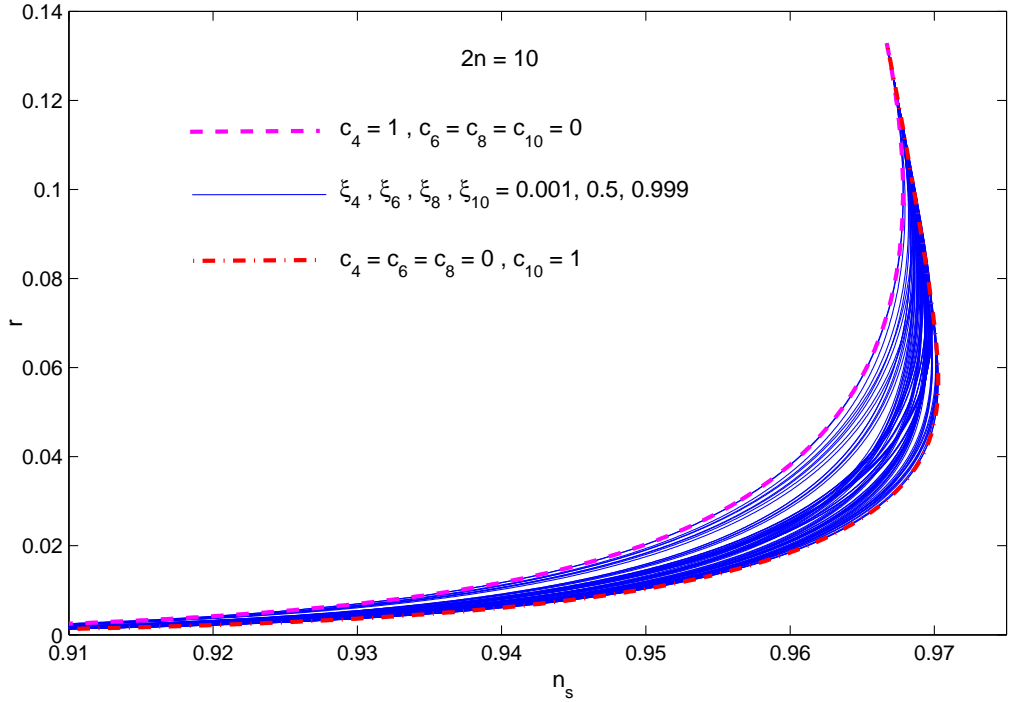


FIG. 2: r vs. n_s for the 10th. order even polynomial potential eq. (3.1) with $n = 5$ and the coefficients c_{2k} taking independently the values indicated. The relation to the numbers ξ_k is given in eq. (3.3). The upper/left border curve $c_4 = 1, c_6 = c_8 = c_{10} = 0$ corresponds to the fourth order potential eq.(2.21). The lower/right border curve $c_{10} = 1, c_4 = c_6 = c_8 = 0$ corresponds to the quadratic plus 10th order term potential eq.(4.1) for $n = 5$. These are the limiting curves of the banana \mathcal{B} region.

We determine the shape of the \mathcal{B} region for arbitrary positive or zero values of the coefficients c_{2k} [subject to the constraint (3.2)], performing a large number of simulations with different setups. After producing coefficients c_{2k} we numerically computed the function $y(u)$ following eq.(2.13)

$$y(u) = 4 \int_u^1 \frac{dx}{x} \frac{1 - x^2 + \sum_{k=2}^n \frac{c_{2k}}{k} (x^{2k} - 1)}{1 - \sum_{k=2}^n c_{2k} x^{2k-2}}$$

and obtain the $r = r(n_s)$ curves from eq. (2.16) by plotting directly r vs. n_s .

Uniform distributions of coefficients are obtained by setting

$$c_{2k} = \left(\sum_{j=1}^n \log \xi_j \right)^{-1} \log \xi_k, \quad k = 1, 2, \dots, n \quad (3.3)$$

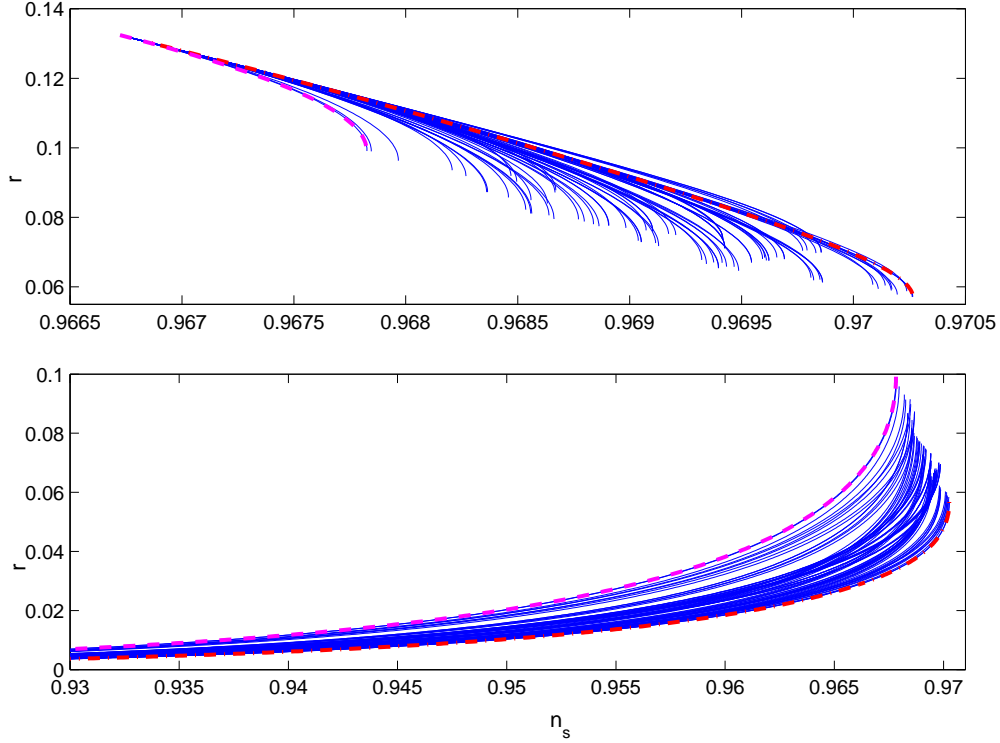


FIG. 3: A detail The banana region \mathcal{B} in the (n_s, r) plane for the quadratic plus 10th order polynomial as in fig. 2, but with the curves split in two parts by the value $r(n_s^{max})$. The upper panel shows the upper branches $r > r(n_s^{max})$ in which r **decreases** with n_s while the lower panel shows the lower branches $r < r(n_s^{max})$ in which r **increases** with n_s . The quadratic plus 10th order polynomial thus provides the **lower border** of the banana region \mathcal{B} setting the lower bound on r . This bound is here $r >$ for the observed allowed range $< n_s <$.

where the numbers ξ_k are independently and uniformly distributed in the unit interval. We used the parametrization eq.(3.3) also when the ξ_k are chosen according to other rules.

For example, in figs. 2-3 we plot the results when $n = 5$, that is for the ten degree polynomial. In this case we let ξ_4, ξ_6, ξ_8 and ξ_{10} take independently the values 0.001, 0.5 or 0.999, for a total of 78 distinct configurations of coefficients. For better clarity, in figs. 2-3 we also include the two border cases $c_4 = 1, c_6 = c_8 = c_{10} = 0$ and $c_{10} = 1, c_4 = c_6 = c_8 = 0$.

For higher values of n we extracted the numbers ξ_k at random within the unit interval. In particular, for the highest case considered, $n = 50$, we used three distributions: in the first, the ξ_k were all extracted independently and uniformly over the unit interval; in the second we set $\log \xi_k = 2^{-k} \log \tilde{\xi}_k$ and extracted the $\tilde{\xi}_k$ independently and uniformly; in the third we picked at random four ξ_k freely varying and fixed to 1 the remaining 45 ones (that is we picked at random four possibly non-zero c_{2k} , setting the rest to zero); the values of the four free ξ_k were chosen at random in the same set of values (0.001, 0.5, 0.999) of the $n = 5$ case. The results of these simulations are shown in fig. 5.

As evident from fig. 3, where the $r = r(n_s)$ curves are split in upper/lower branches with growing/decreasing $r = r(n_s)$ and especially from fig. 5, the case of the quadratic plus $2n$ th order polynomial provides a bound to the banana region \mathcal{B} from below. That is, for any fixed value of n_s , the quadratic plus $2n$ th order polynomial provides the **lowest** value for r .

One sees from fig. 5 that some blue curves $r = r(n_s)$ go beyond the slashed red curve $r = r(n_s)$ for the quadratic plus u^{100} potential on the right upper border of the banana region \mathcal{B} . Namely, the right upper border of the \mathcal{B} region is not given by the quadratic plus u^{100} potential while this potential provides the lower border of the \mathcal{B} region.

We performed many other tests with intermediate values of n and several other distributions, including other k -dependent distributions, with characteristic values for c_{2k} growing linearly with k or decreasing in a power-like or exponential way. In all cases, the results were consistent with those given above.

It is also important to observe that the class of potentials considered, that is arbitrary even polynomials with positive or zero couplings, is a class of weakly coupled models. This is evident from fig. 4, where n_s is plotted vs. the coupling y , which remains of order one when n_s decreases well below the current experimental limits. This weak coupling is the reason why the addition of higher even monomials to these potentials causes only minor quantitative changes to the shape of the $r = r(n_s)$ curves.

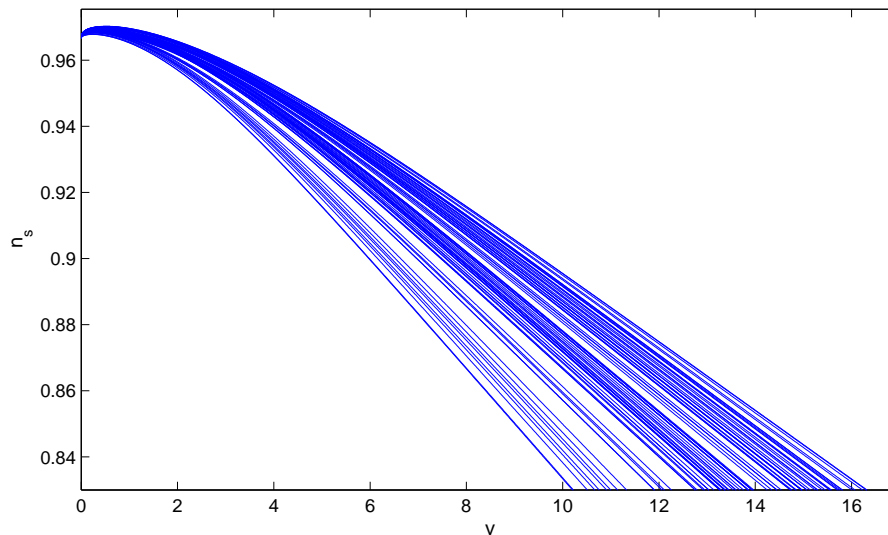


FIG. 4: n_s vs. the coupling y within the same setup as in fig. 2.

The inflaton potential $V(\varphi)$ eq.(3.1) in the original inflaton field φ takes therefore the form

$$V(\varphi) = \frac{4 N M^4}{y(u)} \left\{ 1 - \frac{y(u)}{8 N} \frac{\varphi^2}{M_{Pl}^2} + \sum_{k=2}^n \frac{c_{2k}}{k} \left(\frac{y(u)}{8 N} \right)^k \frac{\varphi^{2k}}{M_{Pl}^{2k}} \right\} ,$$

Therefore, since the coupling $y(u)$ is $\mathcal{O}(1)$ we have the $2k$ -th term in the potential suppressed by the $2k$ -th power of M_{Pl} as well as by the factor $N^k \sim 60^k$.

In particular, the quartic term

$$\frac{y(u) c_4}{32 N} \left(\frac{M}{M_{Pl}} \right)^4 \varphi^4$$

possesses a very small quartic coupling since $M \ll M_{Pl}$. Notice that these suppression factors are natural in the GL approach and come from the ratio of the two relevant energy scales here: the Planck mass and the inflation scale M . When the GL approach is not used these suppression factors do not follow in general.

The validity of the GL approach relies on the wide separation between the scale of inflation and the higher energy scale M_{Pl} (corresponding to the underlying unknown microscopic theory as discussed in ref. [5].) It is not necessary to require $\varphi \ll M_{Pl}$ in the GL approach but to impose [5]

$$V(\varphi) \ll M_{Pl}^4 \quad \text{and hence} \quad v_1(\phi \sqrt{g}) \ll 10^{12} g .$$

This last condition gives an upper bound for the inflaton field φ depending on the large argument behavior of $v_1(u)$. We get for example:

$$\varphi \ll 10^6 M_{Pl} \quad \text{for} \quad v_1(u) \stackrel{u \rightarrow \infty}{\sim} u^2 \quad , \quad \varphi \ll 2600 M_{Pl} \quad \text{for} \quad v_1(u) \stackrel{u \rightarrow \infty}{\sim} u^4 .$$

The validity of the effective GL theory relies on that separation of scales and the GL approach allows to determine the scale of inflation as 0.543×10^{16} GeV (at the GUT scale) and well below the Planck scale M_{Pl} using the amplitude of the scalar fluctuations from the CMB data [6, 7].

Inflaton potentials containing terms of arbitrary high order in the inflaton are considered in ref. [13], sec. 25.3.2 without using the GL approach and within the small field hypothesis $\varphi \ll M_{Pl}$. Smallness conditions on the expansion coefficients are required in ref. [13]. This is actually not needed in the GL approach, whose validity relies only on the wide separation of scales between M and M_{Pl} , at least in the case of even polynomials with positive coefficients.

IV. THE QUADRATIC PLUS THE $2n$ TH ORDER DOUBLE-WELL INFLATON POTENTIAL

In order to find the observationally interesting right and down border of the banana we consider the quadratic plus the $2n$ th order potential for new inflation [10],

$$v_1(u) = \frac{1}{2} (1 - u^2) + \frac{1}{2n} (u^{2n} - 1) . \quad (4.1)$$

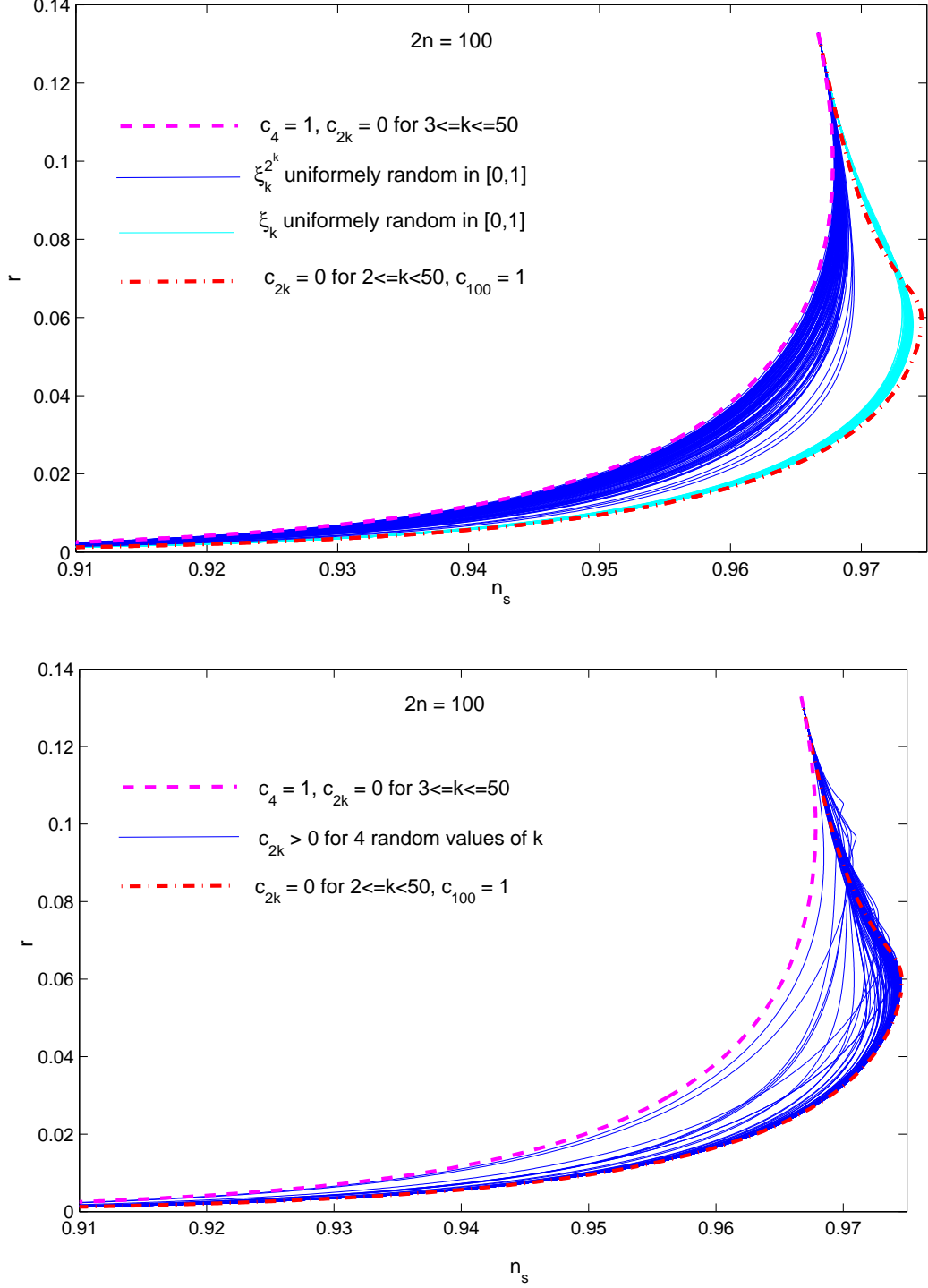


FIG. 5: r vs. n_s for the 100th. order polynomial potential eq.(3.1) for $n = 50$. The coefficients c_{2k} were chosen or extracted at random as indicated in the two panels. The two border curves of the banana region \mathcal{B} are clearly indicated. The upper border is the fourth order potential eq.(2.21) and the lower border is the quadratic plus the $2n$ th order potential eq.(4.1). The quadratic plus the $2n$ th order potential always provides the lowest value for r at any fixed n_s in its lower branch. In the upper panel, all the coefficients c_{2k} were extracted independently from a flat distribution ranging from 0 to 100; in this case the curves **accumulate** near the quadratic plus quartic potential eq.(2.21). The upper panel is the **generic** case. In the lower panel, we picked at random four possibly non-zero c_{2k} and fixed to zero the remaining 44 ones; in this case the curves **accumulate** near the quadratic plus $2n$ th order potential eq.(4.1) with $2n = 100$.

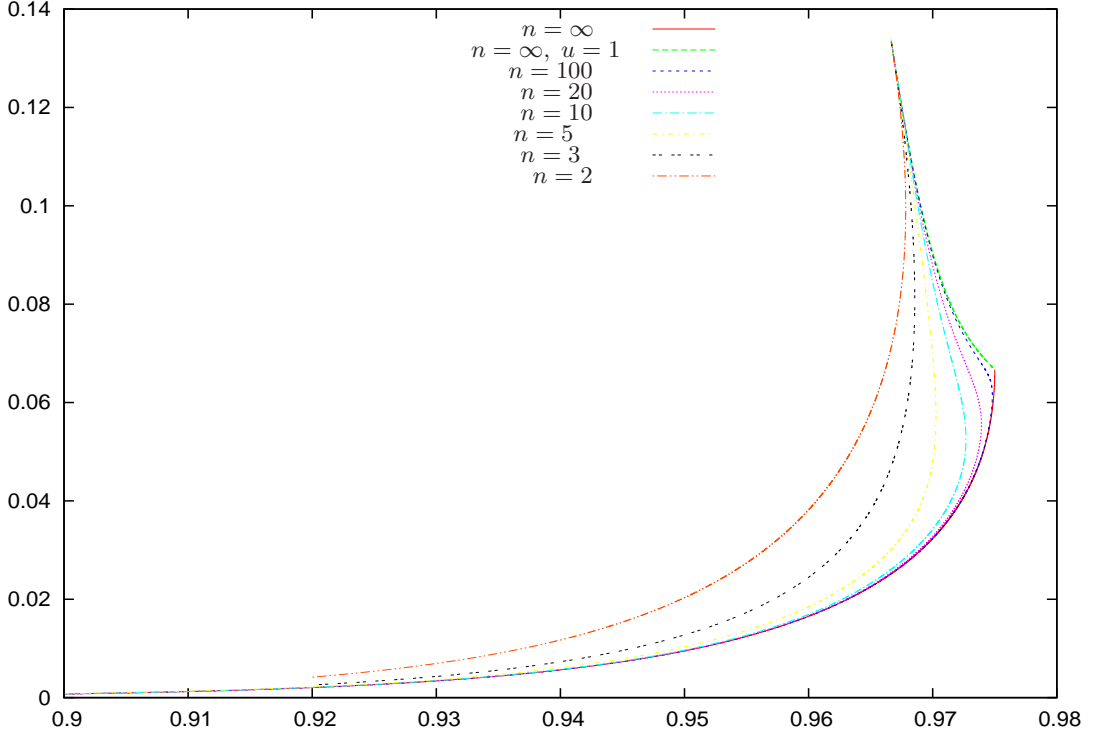


FIG. 6: r vs. n_s for the quadratic plus u^{2n} potential eq.(1.7) setting $N = 60$. The curves for the exponents $n = 2, 3, 5, 10, 20$ and 100 are displayed as well as the limiting curves obtained in the $n = \infty$ limits eqs.(4.6) and (4.11). Eq.(4.6) describes the lower bordering curve while eq.(4.11) describes the upper-right bordering curve. We see that for growing n the curves r vs. n_s tend towards the **limiting** curves. The uppermost point where all curves coalesce corresponds to the monomial quadratic potential $n_s = 0.9666\dots$, $r = 0.13333\dots$ [see eq.(2.25)].

As in the general case eq.(2.10), we choose the absolute minimum at $u = 1$. The customary relation eq.(2.13) takes here the form [10],

$$y(u) = \frac{4}{n} \int_u^1 \frac{dx}{x} \frac{n(1-x^2) + x^{2n} - 1}{1 - x^{2n-2}} \quad \text{where } 0 < u < 1. \quad (4.2)$$

This integral can be expressed as a sum of n terms including logarithms and arctangents [9].

In the weak coupling limit $y \rightarrow 0$, n_s and r take the values of the quadratic monomial potential eqs.(2.17)-(2.18) [7, 10]:

$$n_s - 1 \stackrel{y \rightarrow 0}{\simeq} -\frac{2}{N} = -0.0333\dots, \quad r \stackrel{y \rightarrow 0}{\simeq} \frac{8}{N} = 0.1333\dots, \quad (4.3)$$

while in the strong coupling limit $y \rightarrow \infty$ at fixed n , n_s and r take the values

$$n_s \simeq 1 + \frac{2}{N} \log u \longrightarrow -\infty, \quad r \simeq -\frac{16}{N} \frac{n}{n-1} u^2 \log u \longrightarrow 0^+,$$

in accordance with the general formula eq.(2.19). In fig. 6 we plot r vs. n_s for the potential eq.(4.1) and the exponents $n = 5, 10, 20, 100, 500$ and 5000 . We see that for $n \rightarrow \infty$, r vs. n_s tends towards a **limiting** curve. For $y \rightarrow 0$ we reach the upper end of the curve [the monomial quadratic potential eq.(4.3)] while for large y the left and lower end of the curve is reached. However, the current CMB-LSS data rule out this strong coupling part of the curve for $n_s < 0.95$.

A. The $n \rightarrow \infty$ limit at fixed u .

Let us first compute $y(u)$ eq.(4.2) for $n \rightarrow \infty$ at **fixed** u . Since $0 < x < 1$ in the integrand of eq.(4.2),

$$\lim_{n \rightarrow \infty} x^{2n} = 0.$$

and eq.(4.2) reduces to

$$y(u) \stackrel{n \rightarrow \infty}{\cong} \frac{4}{n} \int_u^1 \frac{dx}{x} [n(1-x^2) - 1] = 2 \left[u^2 - 1 - \ln u^2 + \mathcal{O}\left(\frac{1}{n}\right) \right].$$

Hence, eq.(4.2) becomes

$$y(u) \stackrel{n \rightarrow \infty}{\cong} 2(-\ln u^2 - 1 + u^2) \quad \text{where } 0 < u < 1 \quad \text{and} \quad 0 < y < +\infty. \quad (4.4)$$

which is just twice the result found in the quartic double-well potential, eq. (2.22). Notice that $v_1(u)$ eq.(4.1) in the $n \rightarrow \infty$ limit becomes

$$\lim_{n \rightarrow \infty} v_1(u) = \begin{cases} \frac{1}{2}(1-u^2) & \text{for } u < 1 \\ +\infty & \text{for } u > 1. \end{cases}. \quad (4.5)$$

From eqs.(2.16), (4.1) and (4.4) we find for r and n_s in the $n \rightarrow \infty$ limit

$$\begin{aligned} n_s - 1 &\stackrel{n \rightarrow \infty}{\cong} -\frac{1}{N} \frac{2u^2 + 1}{(1-u^2)^2} (-\ln u^2 - 1 + u^2), \\ r &\stackrel{n \rightarrow \infty}{\cong} \frac{8}{N} \frac{u^2}{(1-u^2)^2} (-\ln u^2 - 1 + u^2). \end{aligned} \quad (4.6)$$

Now, in the limiting cases $u \rightarrow 0$ and $u \rightarrow 1$ (**at** $n = \infty$), that is, the strong coupling limit $y \rightarrow \infty$ and the weak coupling limit $y \rightarrow 0$, respectively, we obtain from eqs.(4.6)

$$\begin{aligned} \lim_{u \rightarrow 1} n_s(n = \infty) - 1 &= -\frac{3}{2N} = -\frac{1}{40} = -0.025, \quad \lim_{u \rightarrow 1} r(n = \infty) = \frac{4}{N} = \frac{1}{15} = 0.0666\dots, \\ \lim_{u \rightarrow 0} n_s(n = \infty) &= -\infty, \quad \lim_{u \rightarrow 0} r(n = \infty) = 0. \end{aligned} \quad (4.7)$$

However, as explained in sec. II, the slow-roll expansion is no more valid when $|n_s - 1| \gtrsim 1$. Moreover, the WMAP+LSS results exclude $n_s \lesssim 0.9$ [1]. Therefore, the limit $u \rightarrow 0$ is ruled out.

Eqs.(4.6) describe the rightmost (limiting) curve in fig. 6 in its **lower** part, namely $0 < r < 4/N = 0.0666\dots$. The upper part is obtained in the double limit $n \rightarrow \infty$ **and** $u \rightarrow 1$ (or, equivalently $n \rightarrow \infty$ **and** $y \rightarrow 0$), as we show in the next section.

B. The double limit $n \rightarrow \infty$ and $u \rightarrow 1$.

As we can see from fig. 6, when y varies from zero to infinity at fixed n , the potential eq.(4.1) covers the region

$$0 < r < \frac{8}{N},$$

the point $r = 8/N$ corresponding to the small coupling limit $y = 0$.

Notice however that the $n \rightarrow \infty$ limit eqs.(4.4) and (4.6) **only** describe the region $0 < r < 4/N$. In order to also describe the small coupling region $8/N > r > 4/N$ for $n \rightarrow \infty$, we have to take in eq.(4.2) the **double** limit $u \rightarrow 1$ **and** $n \rightarrow \infty$. This can be achieved by changing the integration variable in eq.(4.2) as $x = t^{\frac{1}{2n}}$,

$$y(u) = \frac{2}{n^2} \int_{\tau}^1 \frac{dt}{t} \frac{n(1-t^{\frac{1}{n}}) + t - 1}{1 - t^{1-\frac{1}{n}}} \quad \text{where } \tau \equiv u^{2n}, \quad 0 < \tau < 1.$$

Letting $n \rightarrow \infty$ at **fixed** τ yields,

$$\frac{n^2}{2} y(u) \stackrel{n \rightarrow \infty, u \rightarrow 1}{\cong} \int_{\tau}^1 \frac{dt}{t} \frac{t - 1 - \ln t}{1 - t} = \ln \tau + \frac{1}{2} \ln^2 \tau + \text{Li}_2(1 - \tau), \quad (4.8)$$

where

$$\text{Li}_2(s) = - \int_0^s \frac{dt}{t} \ln(1 - t),$$

is the dilogarithmic function [9].

Then, in this **double limit** $n \rightarrow \infty$, $u \rightarrow 1$ eq.(4.2) becomes

$$\gamma^2(\tau) \equiv \frac{n^2}{2} y(u) \stackrel{n \rightarrow \infty, u \rightarrow 1}{\cong} \ln \tau + \frac{1}{2} \ln^2 \tau + \text{Li}_2(1 - \tau) . \quad (4.9)$$

That is, τ and γ^2 **are fixed** in this $n \rightarrow \infty$, $u \rightarrow 1$ limit. Notice that $0 < \tau < 1$, $0 < \gamma < \infty$ while $y \rightarrow 0$

$$y(u) \stackrel{n \rightarrow \infty, u \rightarrow 1}{\cong} \frac{2 \gamma^2(\tau)}{n^2} \rightarrow 0 \quad \text{and} \quad u = \tau^{\frac{1}{2n}} \stackrel{n \rightarrow \infty}{\cong} 1 + \mathcal{O}\left(\frac{1}{n}\right) . \quad (4.10)$$

From eq.(2.16) the spectral index n_s , and the ratio of tensor to scalar fluctuations r for fixed γ and τ take here ($n = \infty$, $y = 0$ and $u = 1$) the following form,

$$\begin{aligned} n_s - 1 &\stackrel{n \rightarrow \infty, u \rightarrow 1}{\cong} -\frac{3 \gamma^2(\tau)}{N} \frac{(1 - \tau)^2}{(\tau - 1 - \ln \tau)^2} + \frac{2 \gamma^2}{N} \frac{\tau}{\tau - 1 - \ln \tau} , \\ r &\stackrel{n \rightarrow \infty, u \rightarrow 1}{\cong} \frac{8 \gamma^2(\tau)}{N} \frac{(1 - \tau)^2}{(1 - \tau + \ln \tau)^2} . \end{aligned} \quad (4.11)$$

We obtain from eqs.(4.11) in the limiting cases $\tau \rightarrow 0$ and $\tau \rightarrow 1$,

$$\begin{aligned} \lim_{\tau \rightarrow 0} n_s - 1 &= -\frac{3}{2N} = -\frac{1}{40} = -0.025 \quad , \quad \lim_{\tau \rightarrow 0} r = \frac{4}{N} = \frac{1}{15} = 0.0666\dots , \\ \lim_{\tau \rightarrow 1} n_s - 1 &= -\frac{2}{N} = -\frac{1}{30} = -0.0333\dots \quad , \quad \lim_{\tau \rightarrow 1} r = \frac{8}{N} = \frac{2}{15} = 0.1333\dots \end{aligned} \quad (4.12)$$

Notice that n_s and r for $n \rightarrow \infty$ and **then** $u \rightarrow 1$ eq.(4.7) coincides with r and n_s in the double limit $n \rightarrow \infty$, $u \rightarrow 1$ for $\tau = u^{2n} \rightarrow 0$ eq.(4.12). Namely, eqs.(4.6) and (4.11) match to each other as eqs.(4.7) and (4.12).

Eqs.(4.11) describe the rightmost (limiting) curve in fig. 6 in its **upper** part, namely $8/N = 0.1333\dots > r > 4/N = 0.0666\dots$. The lower part, $0 < r < 4/N = 0.0666\dots$, is described by eqs.(4.6). r and n_s given by eqs.(4.6) and (4.11) continuously match at $n_s = 0.975$, $r = 0.0666\dots$. However, the derivative dr/dn_s is discontinuous at this point.

There is here a quadratic relation between n_s and r for $r \rightarrow 4^-/N$ valid in the $n = \infty$ limit:

$$\left(r - \frac{4}{N}\right)^2 = -\frac{64}{3N} \left(n_s - 1 + \frac{3}{2N}\right) \left[1 + \mathcal{O}\left(\sqrt{n_s - 1 + \frac{3}{2N}}\right)\right] . \quad (4.13)$$

From eqs.(4.13) and (4.11) we get respectively

$$\lim_{r \rightarrow 4^-/N} \frac{dr}{dn_s} = +\infty \quad , \quad \lim_{r \rightarrow 4^+/N} \frac{dr}{dn_s} = -\frac{8}{3} ,$$

as we can see in fig. 6.

V. THE QUADRATIC PLUS THE EXPONENTIAL POTENTIAL.

Since the exponential function contains all powers of the variable, it is worthwhile to consider it. As before, we restrict ourselves to potentials even in u :

$$v(\phi) = \frac{c_0}{\hat{g}} - \frac{1}{2} \phi^2 + \frac{1}{2\hat{g}c} \left(e^{\hat{g}\phi^2} - 1 - \hat{g}\phi^2\right) , \quad (5.1)$$

where $\hat{g} > 0$ and $c > 0$ are free parameters, while as usual c_0 ensures that $v(\phi)$ vanishes at its absolute minimum $\phi = \phi_{min} = 1/\sqrt{g}$. We find

$$\phi_{min} = \frac{1}{\sqrt{g}} = \sqrt{\frac{1}{\hat{g}} \log(1 + c)} \quad , \quad b \equiv \frac{1}{2} \log(1 + c) > 0 \quad , \quad g = \frac{\hat{g}}{2b}$$

and

$$c_0 = \frac{1}{2} \left[\left(1 + \frac{1}{c}\right) \log(1 + c) - 1 \right]$$

In terms of the variable $u = \phi/\phi_{min}$ the potential $v_1(u)$ defined in general by eq.(2.3) takes here the form,

$$v_1(u) = \frac{e^{-2b(1-u^2)} - 1 + 2b(1-u^2)}{4b(1-e^{-2b})}. \quad (5.2)$$

Expanding the potential eq.(5.2) in powers of u yields

$$v_1(u) \stackrel{u \rightarrow 0}{\cong} \frac{1 + e^{2b}(2b-1)}{4b(e^{2b}-1)} - \frac{1}{2}u^2 + \frac{b}{2(e^{2b}-1)}u^4 + \mathcal{O}(u^6).$$

It is interesting to expand the potential in powers of b in order to make contact with the polynomial potentials of sec. II A-II B. We get from eq.(5.2)

$$v_1(u) \stackrel{b \rightarrow 0}{\cong} \frac{1}{12}(1-u^2)^2(3+b+2bu^2) + \mathcal{O}(b^2)$$

which is exactly the fourth order double-well potential eq.(2.21) to zeroth order in b and the sixth-order double-well potential eq.(2.29) to first order in b .

The field u at horizon exit follows from the customary eq.(2.13) which takes here the form:

$$y(u) = \frac{2}{b} \int_1^u \frac{dx}{x} \frac{e^{-2b(1-x^2)} + 2b(1-x^2) - 1}{e^{-2b(1-x^2)} - 1}, \quad (5.3)$$

Changing the integration variable to $w \equiv 1 - e^{-2b(1-x^2)}$, eq.(5.3) becomes

$$y(u) = 2(-\ln u^2 - 1 + u^2) + \frac{2}{b} \ln u - \frac{1}{b} \int_0^{1-e^{-2b(1-u^2)}} \frac{dw}{w} \frac{\log(1-w)}{2b + \log(1-w)}. \quad (5.4)$$

The spectral index n_s , and the ratio r are expressed from eq.(2.16) as,

$$\begin{aligned} n_s - 1 &= -\frac{3}{8}r + \frac{b y(u)}{N} \frac{(4b u^2 + 1) e^{-2b(1-u^2)} - 1}{e^{-2b(1-u^2)} + 2b(1-u^2) - 1}, \\ r &= \frac{16b^2}{N} u^2 y(u) \left[\frac{e^{-2b(1-u^2)} - 1}{e^{-2b(1-u^2)} + 2b(1-u^2) - 1} \right]^2. \end{aligned} \quad (5.5)$$

We study below eqs.(5.4)-(5.5) in the $b \rightarrow \infty$ limit in the two regimes: $b \rightarrow \infty$ with u **fixed** and $b \rightarrow \infty$ **with** $u \rightarrow u_{min} = 1$. These are the limits investigated in secs. IV A and IV B for the quadratic plus u^{2n} potential, respectively.

In fig. 7 we plot r vs. n_s for the quadratic plus exponential potential eq.(5.1) and the values of the coefficient $c = 0.1, 0.5, 1, 5, \text{ and } 10$. We see that for growing c , r vs. n_s tends towards a **limiting** curve. This curve is the **lower** border of the banana shaped region \mathcal{B} . The upper border is determined by the fourth order potential eq.(2.21).

A. The limit $b \rightarrow \infty$ at fixed u .

For large b we have in eqs.(5.4)-(5.5),

$$e^{-2b(1-u^2)} \ll 1 \quad \text{since } b \gg 1 \quad \text{and } u < 1,$$

and we find

$$\begin{aligned} v_1(u) &\stackrel{b \rightarrow \infty}{\cong} \frac{1}{2}(1-u^2) + \mathcal{O}\left(\frac{1}{b}\right) \quad \text{for } u < 1, \\ \lim_{n \rightarrow \infty} v_1(u) &= +\infty \quad \text{for } u > 1, \\ y(u) &\stackrel{b \rightarrow \infty}{\cong} 2(-\ln u^2 - 1 + u^2) + \mathcal{O}\left(\frac{1}{b}\right), \\ n_s - 1 &\stackrel{b \rightarrow \infty}{\cong} -\frac{1}{N} \frac{2u^2 + 1}{(1-u^2)^2} (-\ln u^2 - 1 + u^2) + \mathcal{O}\left(\frac{1}{b}\right), \\ r &\stackrel{b \rightarrow \infty}{\cong} \frac{8}{N} \frac{u^2}{(1-u^2)^2} (-\ln u^2 - 1 + u^2) + \mathcal{O}\left(\frac{1}{b}\right). \end{aligned} \quad (5.6)$$

These equations for r vs. n_s exactly **coincide** with eqs.(4.5)-(4.6) for the quadratic plus $2n$ th order potential. We have therefore proved that the quadratic plus the u^{2n} potential and the quadratic plus exponential potential have **identical** limits letting $n \rightarrow \infty$ in the former and $b \rightarrow \infty$ in the latter, keeping always u fixed.

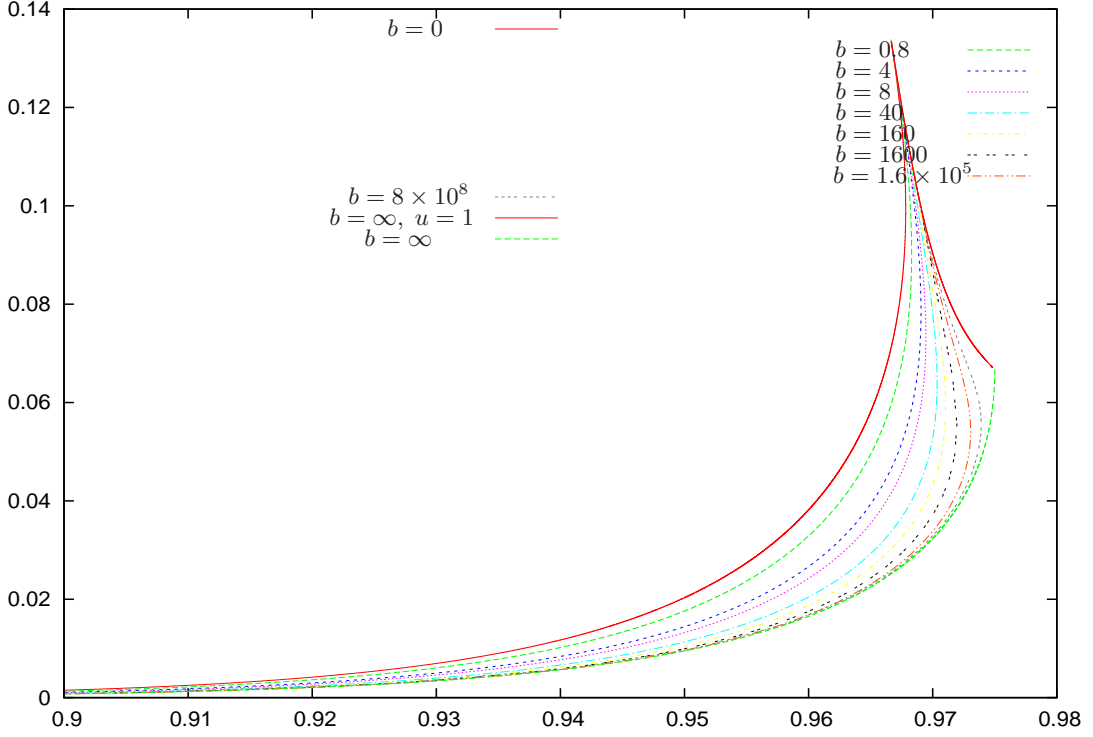


FIG. 7: r vs. n_s for the quadratic plus exponential potential eq.(5.1) with the coefficient $0 \leq b \leq \infty$ and setting $N = 60$. We see that for growing $b \gg 1$, r vs. n_s tends towards a **limiting curve** to the right and down of the banana shaped region \mathcal{B} . This curve is the lower border of the region \mathcal{B} . The upper border is determined by the fourth order potential eq.(2.21). The uppermost point where all curves coalesce corresponds to the monomial quadratic potential $n_s = 0.9666\dots$, $r = 0.13333\dots$ [see eq.(2.25)].

B. The double limit $b \rightarrow \infty$ and $u \rightarrow 1$.

It is useful to introduce here the variable

$$\tau \equiv e^{-2b(1-u^2)} \quad \text{hence} \quad u^2 = 1 + \frac{\log \tau}{2b} \rightarrow 1^- \quad \text{for} \quad b \rightarrow \infty \quad \text{at fixed } \tau, \quad 0 < \tau < 1.$$

We then find from eq.(5.4) for $b \rightarrow \infty$ and fixed τ ,

$$\begin{aligned} 2b^2 y(u) &= 2(-\ln u^2 - 1 + u^2) + \frac{2}{b} \ln u - \frac{1}{2b^2} \int_0^{1-\tau} \frac{dw}{w} \log(1-w) + \mathcal{O}\left(\frac{1}{b}\right) = \\ &= \ln \tau + \frac{1}{2} \ln^2 \tau + \text{Li}_2(1-\tau) + \mathcal{O}\left(\frac{1}{b}\right), \end{aligned} \quad (5.7)$$

We find in this limit from eq.(5.5) for r vs. n_s ,

$$\begin{aligned} r &\stackrel{b \rightarrow \infty, u \rightarrow 1}{=} \frac{8\gamma^2(\tau)}{N} \frac{(1-\tau)^2}{(1-\tau + \ln \tau)^2}, \\ n_s - 1 &\stackrel{b \rightarrow \infty, u \rightarrow 1}{=} -\frac{3\gamma^2(\tau)}{N} \frac{(1-\tau)^2}{(\tau - 1 - \ln \tau)^2} + \frac{2\gamma^2(\tau)}{N} \frac{\tau}{\tau - 1 - \ln \tau}, \\ \gamma^2(\tau) &\equiv 2c^2 y(u) \stackrel{b \rightarrow \infty, u \rightarrow 1}{=} \ln \tau + \frac{1}{2} \ln^2 \tau + \text{Li}_2(1-\tau), \end{aligned} \quad (5.8)$$

where we keep **fixed** γ^2 . Eqs.(5.8) **coincide** with eqs.(4.9)-(4.11) for the quadratic plus u^{2n} potential.

These results plus those in sec. V A **prove** that the quadratic plus u^{2n} potential and the quadratic plus exponential potential eq.(5.1) have **identical** limits letting $n \rightarrow \infty$ in the former and $b \rightarrow \infty$ in the latter.

VI. DYNAMICALLY GENERATED INFLATON POTENTIAL FROM A FERMION CONDENSATE IN THE INFLATIONARY STAGE.

The inflaton may be a coarse-grained average of fundamental scalar fields, or a composite (bound state) or condensate of fields with spin, just as in superconductivity. Bosonic fields do not need to be fundamental fields, for example they may emerge as condensates of fermion-antifermion pairs $\langle \bar{\Psi}\Psi \rangle$ in a grand unified theory (GUT) in the cosmological background [7].

We investigate in this section an inflaton potential dynamically generated as the effective potential of fermions in the inflationary universe. We consider the inflaton field coupled to Dirac fermions Ψ through the interaction Lagrangian

$$\mathcal{L} = \bar{\Psi} [i \gamma^\mu \mathcal{D}_\mu - m_f - g_Y \varphi] \Psi . \quad (6.1)$$

Here g_Y stands for a generic Yukawa coupling between the fermions and the inflaton φ . The fermion mass m_f can be absorbed in a constant shift of the inflaton field. The Dirac matrices γ^μ are the curved space-time γ -matrices and \mathcal{D}_μ stands for the fermionic covariant derivative.

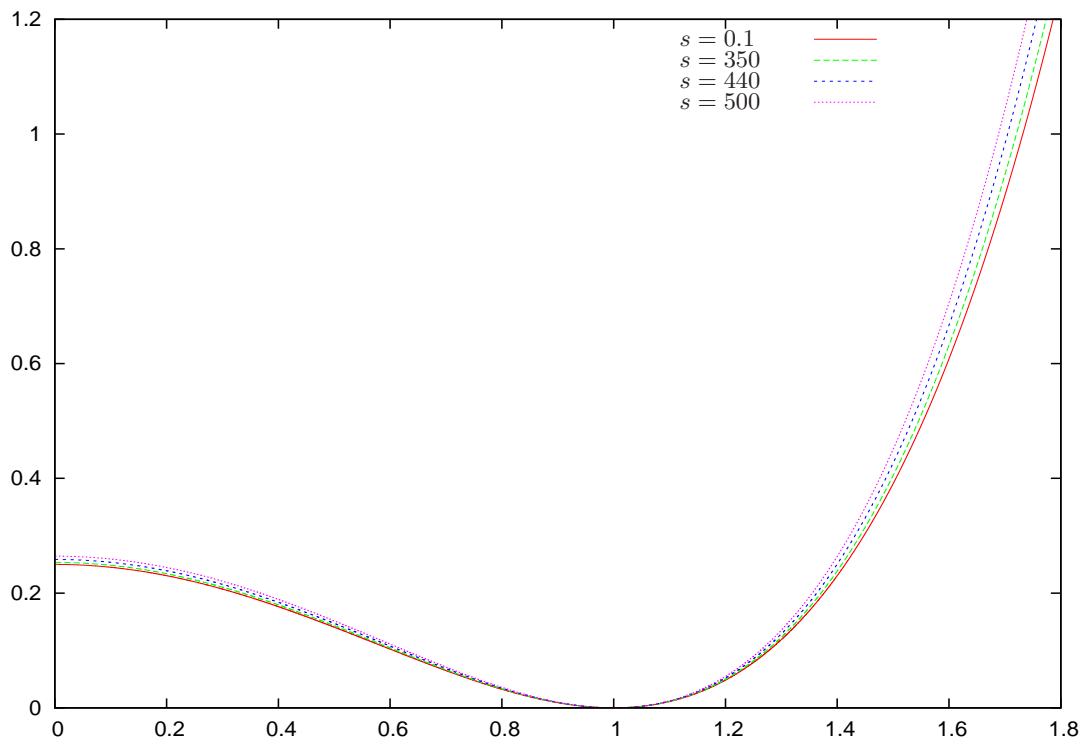


FIG. 8: The effective potential $v_1(u)$ generated from fermions eq.(6.9) vs. u for several values of the rescaled Yukawa coupling s . The steeper potential corresponds to the largest s . The shallower potential corresponds to $s \rightarrow 0$ and it is the quadratic plus quartic potential eq.(2.21).

For our purposes in this section, the inflationary stage can be approximated by a de Sitter space-time (that is, we neglect the slow decrease in time during inflation of the Hubble parameter H). In this way, the effective potential of fermions can be computed in close form with the result [7, 11],

$$V_f(\varphi) = V_0 + \frac{1}{2} \mu^2 \varphi^2 + \frac{1}{4} \lambda \varphi^4 + H^4 Q \left(g_Y \frac{\varphi}{H} \right) , \quad (6.2)$$

where,

$$\begin{aligned} Q(x) &= \frac{x^2}{8\pi^2} \{ (1+x^2) [\gamma + \text{Re} \psi(1+ix)] - \zeta(3)x^2 \} \quad , \quad x \equiv g_Y \frac{\varphi}{H} , \\ &= \frac{x^4}{8\pi^2} \left[(1+x^2) \sum_{n=1}^{\infty} \frac{1}{n(n^2+x^2)} - \zeta(3) \right] \\ &= \frac{x^4}{8\pi^2} \sum_{n=1}^{\infty} (-1)^{n+1} [\zeta(2n+1) - \zeta(2n+3)] x^{2n} . \end{aligned} \quad (6.3)$$

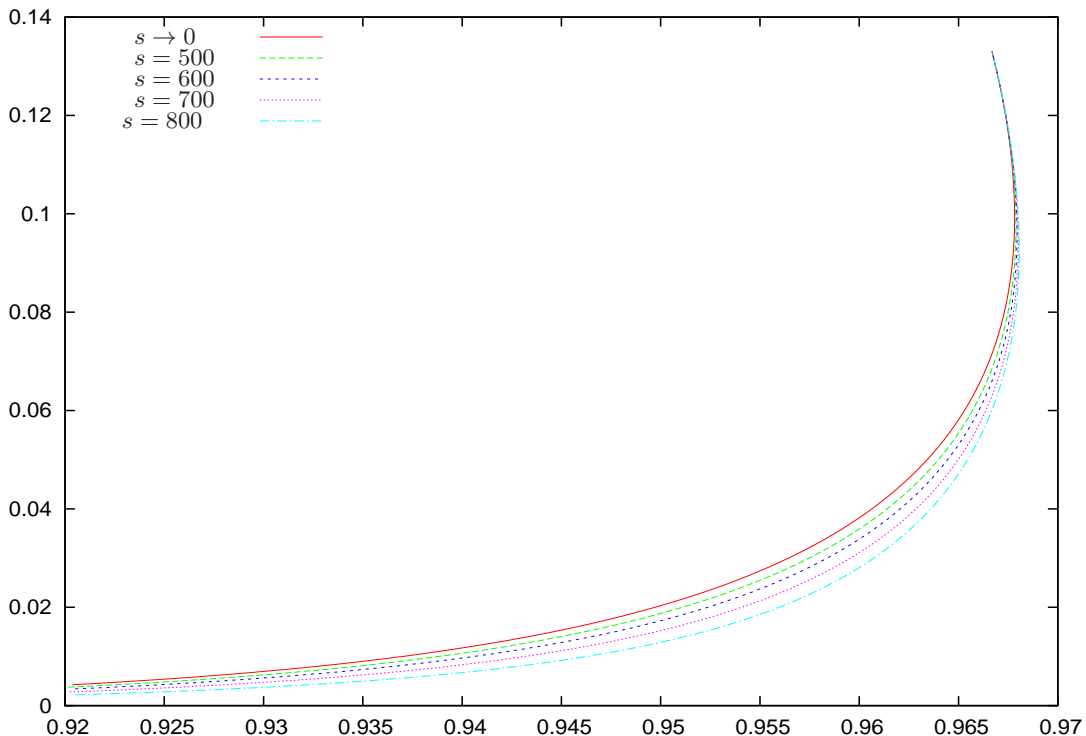


FIG. 9: We plot here r vs. n_s for the effective potential obtained from fermions in de Sitter stage eq.(6.7) for the physical value of the parameter g eq.(6.11). For weak Yukawa coupling $s \ll 1$ we recover the $r = r(n_s)$ curve for the quadratic plus quartic potential eq.(2.21). The $r = r(n_s)$ curves are inside the universal banana region [fig. 10] provided $s \leq 850$, slightly exceeding the bound eq.(6.12).

We included in $V_f(\varphi)$ the renormalized mass μ^2 and renormalized coupling constant λ which are free and finite parameters. $\psi(x)$ stands for the digamma function, γ for the Euler-Mascheroni constant and $\zeta(x)$ for the Riemann zeta function [9].

Eq.(6.2) is the energy density for an homogeneous inflaton field φ coupled to massless fermions through the Lagrangian eq.(6.1) in a de Sitter space-time.

The power series of the function $Q(x)$ has coefficients with alternating signs, but it can be readily verified that $Q(x) > 0$ and $Q'(x) > 0$ for $x > 0$. Moreover, to leading order we have

$$Q(x) \stackrel{x \rightarrow \infty}{\approx} \frac{x^4}{8\pi^2} \left[\log x + \gamma - \zeta(3) + \mathcal{O}\left(\frac{1}{x}\right) \right]. \quad (6.4)$$

The constant V_0 in eq. (6.2) must be such that the potential $V_f(\varphi)$ fulfills eq. (1.6) producing a finite number of inflaton e-folds. We consider new inflation and choose $\mu^2 = -m^2 < 0$. Hence $V_f(\varphi)$ has a double-well shape with the absolute minimum at $\varphi = \varphi_{min}$, with φ_{min} a function of the free parameters of the potential.

Expanding $V_f(\varphi)$ in powers of φ gives

$$V_f(\varphi) = V_0 - \frac{1}{2} m^2 \varphi^2 + \frac{1}{4} \lambda \varphi^4 + \frac{1}{8\pi^2} [\zeta(3) - \zeta(5)] \frac{(g_Y \varphi)^6}{H^2} + \mathcal{O}(g_Y^8 \varphi^8).$$

where $\zeta(3) - \zeta(5) = 0.16513 \dots > 0$.

In the $H \rightarrow 0$ limit, eq.(6.2) becomes the effective potential for fermions in Minkowski space-time [7]. Recall that

$$H = \sqrt{N} \mathcal{H} m \quad , \quad m = \frac{M^2}{M_{Pl}} \quad (6.5)$$

where the dimensionless Hubble parameter \mathcal{H} turns out to be of order one [7].

As in the general description of section II, eq.(2.12) we introduce the dimensionless coupling constant g as

$$g = \frac{M_{Pl}^2}{\varphi_{min}^2}$$

Besides g we can now form two other independent and positive dimensionless shape parameters, that is

$$s \equiv g_Y \frac{\varphi_{min}}{H} = \frac{g_Y}{\sqrt{g}} \frac{M_{Pl}}{H} \quad , \quad q \equiv \frac{H^2}{m \varphi_{min}} = \sqrt{g} \frac{H^2}{m M_{Pl}} = \sqrt{g} \frac{H^2}{M^2} \quad , \quad x = s u . \quad (6.6)$$

We derive the dimensionless potential $v_1(u)$ from eq.(6.2) using the general transformation equations (2.15). We obtain,

$$v_1(u) = \frac{g}{M^4} V_f(\varphi_{min} u) = c_0 - \frac{1}{2} u^2 + \frac{1}{4} c_4 u^4 + \frac{g}{M^4} H^4 Q(s u) \quad (6.7)$$

The parameters c_0 and c_4 are determined by requiring that $v_1(1) = v_1'(1) = 0$ as in sec. II. We thus obtain from eq.(6.7)

$$c_4 = 1 - q^2 s Q'(s) \quad , \quad c_0 = \frac{1}{4} + \frac{1}{4} q^2 s Q'(s) - q^2 Q(s) \quad (6.8)$$

Inserting c_0 and c_4 into eq.(6.7) yields for the inflaton potential

$$\begin{aligned} v_1(u) &= \frac{g}{M^4} V_f(\varphi_{min} u) = \frac{1}{2} (1 - u^2) + \frac{1}{4} [1 - q^2 s Q'(s)] (u^4 - 1) + q^2 [Q(s u) - Q(s)] \\ &= \frac{1}{2} (1 - u^2) + \frac{1}{4} (1 - b) (u^4 - 1) + b F(u, s) , \end{aligned} \quad (6.9)$$

where

$$b \equiv q^2 s Q'(s) \geq 0 \quad , \quad F(u, s) \equiv \frac{Q(s u) - Q(s)}{s Q'(s)} \quad (6.10)$$

Notice that $v_1(u)$ reduces to the quartic double-well potential $\frac{1}{4}(1-u^2)^2$ when $s \rightarrow 0$ at fixed q (that is, when $g_Y \rightarrow 0$) as well as when $b \rightarrow 0$ at fixed s . This last limit means $g_Y \rightarrow 0$ with $g_Y M_{Pl}/H$ fixed.

Only the interval $0 < u < 1$ is relevant for the inflaton evolution. For any u in this interval, $F(u, s)$ is negative definite and is monotonically decreasing as a function of s . In particular,

$$F(u, s) \stackrel{s \rightarrow 0}{\simeq} \frac{1}{6} (u^6 - 1) \quad , \quad F(u, s) \stackrel{s \rightarrow \infty}{\simeq} \frac{1}{4} (u^4 - 1) + \mathcal{O}\left(\frac{1}{\log s}\right) \quad , \quad 0 < u < 1 \text{ fixed}$$

Hence for $s \rightarrow 0$ at fixed b we obtain again the sixth-order double-well potential of eq. (2.29)

$$v_1(u) \longrightarrow \frac{1}{12} (1 - u^2)^2 (3 + b + 2b u^2) \quad , \quad s \rightarrow 0 \text{ at fixed } b \quad ,$$

while b cancels out for large s and we get back the quartic double-well potential

$$v_1(u) \longrightarrow \frac{1}{4} (1 - u^2)^2 \quad , \quad s \rightarrow \infty \text{ at fixed } b \quad .$$

The terms containing Q in the effective potential eqs.(6.2) and (6.9) represent the one-loop quantum contributions. They vanish when $b = 0$ while for $b > 0$ they should be sizably smaller than the tree level contribution, otherwise all higher loops effects must also be taken into account. In particular, the quartic term in eq. (6.9) must have a non-negative coefficient, that is $0 < b \leq 1$ as in sec. II B.

We see from eq.(6.9) that the one-loop (Q) pieces are of the order $q^2 Q(s u)$ compared with the tree-level pieces. We can compute q using eqs.(2.14), (6.5) and (6.6) with the result

$$q = \sqrt{\frac{N y}{8}} \left(\frac{\mathcal{H} M}{M_{Pl}} \right)^2 \simeq 0.854 \cdot 10^{-5} \ll 1 \quad , \quad (6.11)$$

where $y \simeq 1.3$ and $\mathcal{H} \simeq 0.5$ [7].

Hence, the one-loop pieces are negligible unless $s \gg 1$. We can therefore use the asymptotic behavior eq.(6.4) to estimate $Q(s u)$ for large s . In order the one-loop part to be smaller or of the order of the tree level piece we must impose in the strong coupling regime $s \gg 1$,

$$\frac{1}{8 \pi^2} s^4 q^2 \ln s \lesssim 1 \quad \Rightarrow \quad s \lesssim 1020 [\ln 1020]^{-1/4} \simeq 616 \quad . \quad (6.12)$$

The one-loop potential eq.(6.9) is therefore reliable for $s \lesssim 600$. For larger values of s the one-loop piece is larger than the tree level part and hence all higher order loops should be included too.

For $s \sim 1$ we recover the quadratic plus quartic potential eq.(2.21) since the terms in $s^4 q^2$ are negligible in eq.(6.9) and n_s and r are thus given by eqs.(2.23). We find from eqs.(6.9) and (6.11) in the case $s \sim 1$,

$$v_1(u) = \frac{1}{4} - \frac{1}{2} u^2 + \frac{1}{4} u^4 + \mathcal{O}\left(\frac{H^2}{M_{Pl}^2}\right)$$

That is, the terms beyond u^4 in the effective potential from the fermions are of the same order of magnitude as the loop corrections to inflation [7, 18] and can be neglected since $(H/M_{Pl})^2 \sim 10^{-9}$.

We display in fig. 9 r vs. n_s for various values of the Yukawa coupling s . Therefore, the banana region \mathcal{B} in the (n_s, r) plane for the effective potential eq.(6.9) is the region limited by the curves for the potential for $s \leq 500$ and for $s \rightarrow 0$ as displayed in fig. 9. Notice that the lower border of the region \mathcal{B} for the effective potential eq.(6.9) is well **above** the lower border of the universal \mathcal{B} region displayed in fig. 10.

In summary, the $r = r(n_s)$ curves for the dynamically generated inflaton potential eq.(6.9) are **inside** the universal banana region \mathcal{B} for all values of the Yukawa coupling g_Y that keep the result for this one-loop potential reliable. Namely, the one-loop piece is smaller or of the order of the tree level part.

VII. THE UNIVERSAL BANANA REGION \mathcal{B}

In summary, we find that all $r = r(n_s)$ curves for double-well inflaton potentials in the Ginsburg-Landau spirit fall **inside** the **universal** banana region \mathcal{B} depicted in fig. 10 for new inflation. Namely,

- The fourth degree double-well potentials containing a cubic term studied in ref. [6]:

$$v_1(u) = \frac{1}{4} + \frac{\beta}{6} - \frac{1}{2} u^2 - \frac{2}{3} \beta u^3 + \frac{1}{4} (1 + 2\beta) u^4, \quad (7.1)$$

where $\beta \geq 0$ is the asymmetry parameter. This potential reduces to eq.(2.21) for $\beta = 0$.

- The quadratic plus sixth-order potential eq.(2.29).
- The even polynomial potentials with arbitrarily higher-order degrees and positive coefficients (sec. III).
- The quadratic plus exponential potential (sec. V).
- The inflaton potential dynamically generated from fermions (sec. VI).

Potentials in the Ginsburg-Landau spirit have usually coefficients of order one when written in dimensionless variables. This is the case of the inflaton potentials $v_1(u)$. In that case, we found that all $r = r(n_s)$ curves for double-well potentials fall **inside** the universal banana region \mathcal{B} depicted in fig. 10. Moreover, for even double-well potentials with arbitrarily large positive coefficients, their $r = r(n_s)$ curves lie inside the universal banana region \mathcal{B} [fig. 10].

The study of the dynamically-generated inflaton potential in sec. VI leads to analogous conclusions. This one-loop inflaton potential is reliable as long as the one-loop piece is smaller or of the same order than the tree level part. In such regime all the curves $r = r(n_s)$ produced by this fermion-generated potential lie **inside** the universal banana region \mathcal{B} .

More generally, we see from eq.(2.20) that $r \ll 1$ is generally linked to a large coupling $y \gg 1$. However, this strong coupling regime corresponds to n_s values well below the current best observed value $n_s = 0.964$, and is therefore excluded by observations.

The lower border of the universal region \mathcal{B} corresponds to the limit binomial potential eq.(4.5)

$$v_1(u) = \frac{1}{2} (1 - u^2) \quad \text{for } u < 1 \quad , \quad v_1(u) = +\infty \quad \text{for } u > 1 .$$

and is described parametrically by eq.(4.6). We obtain such potential and such parametrization of $r = r(n_s)$ both as the $n \rightarrow \infty$ limit of the quadratic plus u^{2n} potential in sec. IV as well as the $b \rightarrow \infty$ limit of the $e^{2bg\phi^2}$ potential in sec V.

The upper-right border of the universal banana-shaped region \mathcal{B} is not given by eqs.(4.9) and (4.11) corresponding to the double limit $n \rightarrow \infty$ and $u \rightarrow 1$ (or, alternatively $b \rightarrow \infty$ and $u \rightarrow 1$). This follows from the fact that some potentials of order 100 yield $r = r(n_s)$ curves above the limiting curves for the quadratic plus u^{100} potential as depicted in fig. 5.

The upper-left border of the universal region \mathcal{B} depicted in fig. 10 is given by the fourth order double-well potential eq.(2.21) and it is described parametrically by eq.(2.23).

The lower border of the universal region \mathcal{B} is particularly relevant since it gives a **lower bound** for r for each observationally allowed value of n_s . For example, the best n_s value $n_s = 0.964$ implies from fig. 10 that $r > 0.021$.

The upper border of the universal region \mathcal{B} tells us the upper bound $r < 0.053$ for $n_s = 0.964$. Therefore, we have within the large class of potentials inside the region \mathcal{B}

$$0.021 < r < 0.053 \quad \text{for} \quad n_s = 0.964. \quad (7.2)$$

Notice that these bounds on r are compatible with the experiments [1].

The Ginsburg-Landau criterion applied to the inflaton potential eq.(2.11) leads to values of (n_s, r) inside the universal banana-shaped region \mathcal{B} . In principle, within the Ginsburg-Landau approach, one should choose potentials $v_1(u)$ with **small** coefficients $|c_k| \gg 1$ in eq.(2.10). However, as shown in sec. III, this restriction does not apply for double-well potentials of even degree: for this class of potentials **large** and positive coefficients $c_{2k} \gg 1$ also provide (n_s, r) **within** the universal banana region \mathcal{B} . Moreover, the double-well quartic potential eq.(7.1) also provides (n_s, r) inside the banana region \mathcal{B} for arbitrarily large coefficient β [6].

On the contrary, double-well potentials of degree larger than four with large negative coefficients are outside the Ginsburg-Landau class and produce (n_s, r) outside the region \mathcal{B} . In particular, it is possible to produce in this way n_s values compatible with the data together with arbitrarily small values for r by choosing large enough negative coefficients c_k .

We find that the Ginsburg-Landau class of potentials is **physically well motivated** and therefore that the banana-shaped region \mathcal{B} is a natural region to expect to observe (n_s, r) . Namely, taking into account the present data for n_s we expect that r will be observed in the interval eq.(7.2). Anyhow, the fourth order double-well potential eq.(1.7) provides an excellent fit to the present CMB/LSS data and yields as most probable values: $n_s \simeq 0.964$, $r \simeq 0.051$.

The physical framework provided by the Ginsburg-Landau effective theory of inflation allows to take high benefit of the data (of the present data and the forthcoming ones). The lower bounds (and most probable value) we infer for r are the best way to support the searching for CMB polarisation and the future missions on it.

-
- [1] E. Komatsu et al. (WMAP collaboration), *Astrophys. J. Suppl.* **180**:330 (2009).
 G. Hinshaw et al. (WMAP collaboration), *Astrophys. J. Suppl.* **180**:225 (2009).
 M. R.olta et al. (WMAP collaboration), *Astrophys. J. Suppl.* **180**:296 (2009).
 E. Komatsu et al. (WMAP collaboration), arXiv:1001.4538.
- [2] Kolb EW and Turner MS, *The Early Universe*, Addison Wesley. Redwood City, C.A. 1990. Dodelson S, *Modern Cosmology*, Academic Press, 2003.
- [3] See for example: Hu W., Dodelson S., *Ann. Rev. Astron. Ap.* **40**: 171 (2002); Lidsey J, Liddle A, Kolb E, Copeland E, Barreiro T, Abney M, *Rev. of Mod. Phys.* **69**: 373, (1997).
- [4] Statistical Physics, vol 9, E M Lifshitz, L P Pitaevsky, Pergamon Press, Oxford 1980, see secs. 142 part I and 45 part II. L. D. Landau, *Zh. Eksp. Teor. Fiz.*, **7**, 19 (1937) and **7**, 545 (1937) and in *Collected Papers of L. D. Landau*, Pergamon Press, Oxford, 1965. V. L. Ginsburg, *Zh. Eksp. Teor. Fiz.* **15**, 739 and **10**, 107 (1945). V. L. Ginsburg, L. D. Landau, *Zh. Eksp. Teor. Fiz.* **20**, 1064 (1950). V. L. Ginsburg, *About Science, Myself and Others*, Part I, Chapters 5-7, IoP, Bristol, 2005.
- [5] D. Boyanovsky, H. J. de Vega, N. G. Sánchez, *Phys. Rev.* **D73**, 023008 (2006).
- [6] C. Destri, H. J. de Vega, N. G. Sánchez, *Phys. Rev.* **D77**, 043509 (2008).
- [7] D. Boyanovsky, C. Destri, H. J. de Vega, N. G. Sánchez, arXiv:0901.0549, *Int. J. Mod. Phys. A* **24**, 3669-3864 (2009).
- [8] F. Finelli, M. Rianna, N. Mandolesi, *JCAP* 0612 (2006) 006. M. Bridges, A.N. Lasenby, M.P. Hobson, *MNRAS*, **369**, 1123 (2006). Hufenberger, K. M. et al. *Ap. J.* **688**, 1 (2008), *Ap. J.* **651**, L81 (2006). H. K. Eriksen et al., *ApJ*, **656**, 641 (2007).
- [9] A. P. Prudnikov, Yu. A. Brichkov, O. I. Marichev, *Integrals and Series*, Nauka, Moscow, 1981.
- [10] D. Boyanovsky, H. J. de Vega, C. M. Ho, N. G. Sánchez, *Phys. Rev.* **D75**, 123504 (2007).
- [11] D. Boyanovsky, H. J. de Vega, N. G. Sánchez, *Phys. Rev.* **D72**, 103006 (2005).
- [12] D. Cirigliano, H. J. de Vega, N. G. Sánchez, *Phys. Rev.* **D 71**, 103518 (2005).
- [13] D. Lyth, A. Liddle, 'The Primordial Density Perturbation', Cambridge University Press, 2009.
- [14] M. B. Hoffman, M. S. Turner, *Phys. Rev.* **D64**, 023506 (2001), W. H. Kinney, *Phys. Rev.* **D66**, 083508 (2002), R. Easther, W. H. Kinney, *Phys. Rev.* **D67**, 043511 (2003). A. Kosowsky, M. S. Turner, *Phys. Rev.* **D52**, R1739 (1995), L. A. Boyle, P. J. Steinhardt, N. Turok, *Phys. Rev. Lett.* **96** (2006) 111301. B. A. Powel, W. H. Kinney, *JCAP* 0708:006, (2007). W. H. Kinney, E. W. Kolb, A. Melchiorri, A. Riotto, *Phys. Rev.* **D74** (2006) 023502. C. Y. Chen et al., *Class. Quant. Grav.* **21**, 3223 (2004). E. Ramirez, A. R. Liddle, *Phys. Rev.* **D71**, 123510 (2005). R. Easther, J. T. Giblin, *Phys. Rev.* **D72**, 103505 (2005). M. Spalinski, *JCAP*0708:016,2007.
- [15] W. H. Kinney, *Phys. Rev.* **D58**, 123506 (1998). C. Savage, K. Freese, W. H. Kinney, *Phys. Rev.* **D74**, 123511 (2006). L. Alabidi, D. Lyth *JCAP* 0605 (2006) 016 and 0608 (2006) 013. L. Boyle, P J Steinhardt, arXiv:0810.2787.
- [16] K. Kadota, E. D. Stewart, *JHEP* (2003) 013. L. Boubekour, D. Lyth *JCAP* 0507 (2005) 010. K. Kohri, C-M Lin, D. Lyth, *JCAP* 0712 (2007) 004. C-M Lin, K. Cheung, *JCAP* 0903 (2009) 012.
- [17] D. Boyanovsky, H. J. de Vega, D. J. Schwarz, hep-ph/0602002, *Ann. Rev. Nucl. Part. Sci.* **56**, 441-500, (2006).
- [18] D. Boyanovsky, H. J. de Vega, N. G. Sánchez, *Nucl. Phys.* **B747**, 25 (2006) and *Phys. Rev.* **D72**, 103006 (2005).
- [19] Kinney, W. H. et al. 2008, *Phys. Rev.* **D78**, 087302.

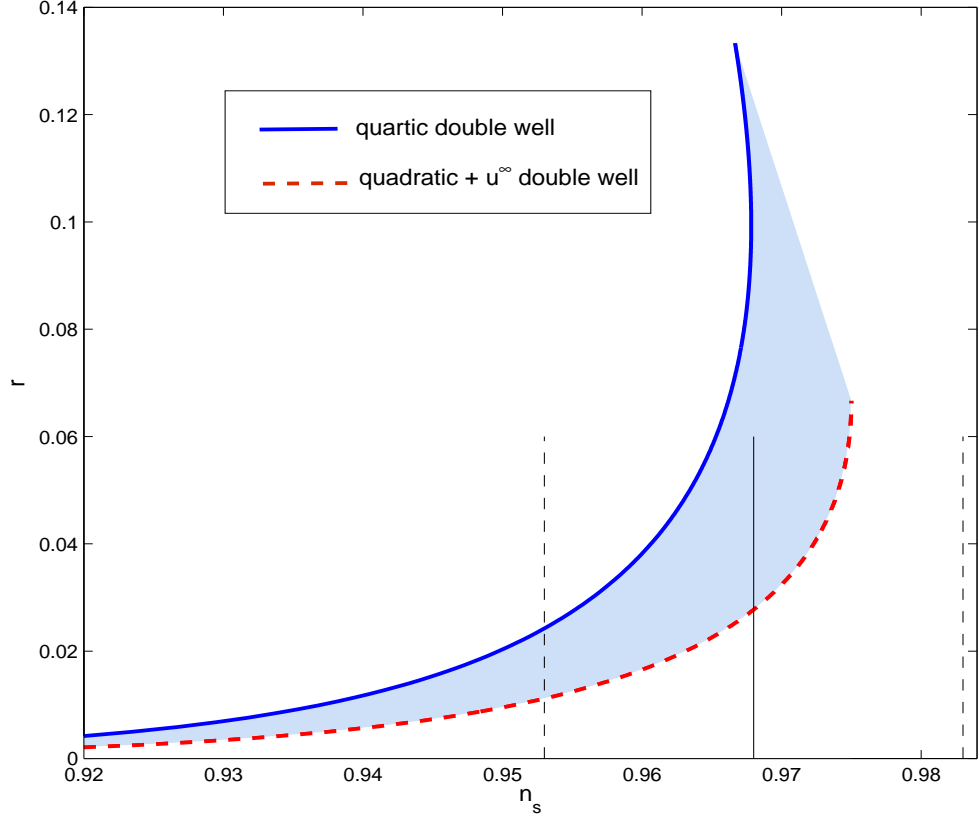


FIG. 10: We plot here the borders of the universal banana region \mathcal{B} in the (n_s, r) -plane setting $N = 60$. The curves are computed with the quadratic plus quartic potential eq.(2.21) and with the $n = \infty$ limit of the quadratic plus u^{2n} potential eq.(4.1) (or the $b = \infty$ limit of the quadratic plus exponential potential eq.(5.1), which gives identical results) as given by eqs.(4.4)-(4.6) and eqs.(4.9) and (4.11). Notice that the lower part of the right border of \mathcal{B} , $0 < r < 4/N = 0.06666\dots$ corresponds to the limit $n = \infty$ at fixed u eq.(4.6). The upper part $4/N < r < 8/N$ of the right border of \mathcal{B} is not displayed here. We display in the vertical full line the LCDM+r value $n_s = 0.968 \pm 0.015$ using WMAP5+BAO+SN data. The broken vertical lines delimit the $\pm 1\sigma$ region.

[20] Peiris H. V. & Easther R., 2008, JCAP 7, 24.

[21] C. Burigana, C. Destri, H. J. de Vega, A. Gruppuso, N. Mandolesi, P. Natoli, N. G. Sanchez, arXiv:1003.6108 to appear in ApJ.